# International Association for Hydraulic Research Working Group on Thermal Regimes
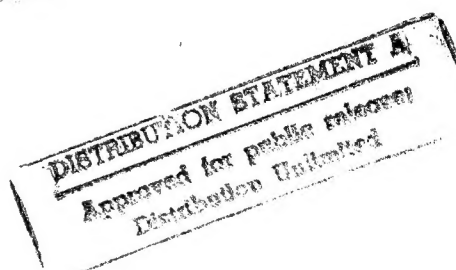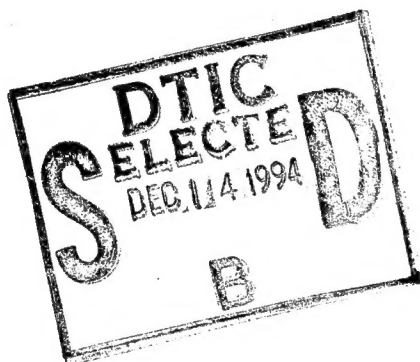# Report on Frazil Ice

Steven F. Daly, Editor

August 1994

DTIC
SELECTED
DEC 1 4 1994
B

DISTRIBUTION STATEMENT A
Approved for public release;
Distribution Unlimited

**19941207 072**

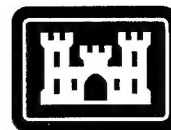DTIC QUALITY INSPECTED 1

IAHR
AIRH

**Abstract**

This report, prepared by members of the Working Group on Thermal Regimes of the Section on Ice Research and Engineering of the International Association for Hydraulic Research, is a comprehensive overview of frazil ice. Starting from the initial nucleation of single frazil ice crystals to the formation of ice covers that may be many kilometers long, the physics and evolution of frazil ice in natural water bodies are described. Laboratory experiments conducted over the last 30 years on frazil ice dynamics and other aspects of frazil are described and classified. A physically based, quantitative model that describes the dynamic evolution of the crystal size distribution function is presented. In addition, the development of numerical models of frazil ice in oceans and rivers is discussed and their results described. This report serves as a review of the state of the art of the present understanding of frazil, and the extensive references are a comprehensive resource.

# Special Report 94-23

## International Association for Hydraulic Research
## Working Group on Thermal Regimes
# Report on Frazil Ice

Steven F. Daly, Editor

August 1994

## PREFACE

This report was prepared by the Working Group on Thermal Regimes of the Section on Ice Research and Engineering of the International Association for Hydraulic Research. It was edited by Steven F. Daly, Research Hydraulic Engineer, Ice Engineering Research Branch, Experimental Engineering Division, U.S. Army Cold Regions Research and Engineering Laboratory; he also contributed several of the chapters herein. Other contributors are Dr. Thomas Forest, Professor of Mechanical Engineering, University of Alberta, Edmonton, Alberta; Dr. Anders Omstedt, Associate Professor, Swedish Meteorological and Hydrological Institute, Norrkoping, Sweden; and Kathleen D. White, Research Hydraulic Engineer, Ice Engineering Research Branch, CRREL.

The contents of this report are not to be used for advertising or promotional purposes. Citation of brand names does not constitute an official endorsement or approval of the use of such commercial products.

# CONTENTS

## ILLUSTRATIONS

Figure

**TABLES**                                                                    Page

Table

v

# CHAPTER 1

# Physics of Frazil Ice

THOMAS FOREST

## NOMENCLATURE

| | |
|---|---|
| $C_o$ | molar concentration dissolved in liquid |
| $L$ | latent heat of fusion |
| $R$ | universal gas constant |
| $R_c$ | critical radius |
| $T_i$ | interface temperature |
| $T_\infty$ | liquid temperature |
| $T_m$ | freezing point of liquid |
| $T_o$ | freezing point of pure liquid |
| $\Delta T$ | $T_m - T_\infty$ |
| $\Delta T_i$ | interface supercooling |
| $\Delta T_m$ | $T_o - T_m$ |
| $v_s$ | specific volume of solid |
| $v$ | growth velocity |
| $\alpha$ | solid/liquid interface roughness |
| $\gamma$ | surface free energy |
| $\varepsilon$ | fraction of binding energy associated with crystal face |
| $\mu_1, \mu_2, \mu_3$ | constants |

## INTRODUCTION

The formation and evolution of "frazil" ice in turbulent water that undergoes a small degree of supercooling is a problem that involves several fundamental aspects. The important questions regarding the basic physics of the process are:

1. How do frazil ice crystals originate?
2. What shape do frazil crystals adopt and why?
3. How is the size of frazil crystals related to the thermodynamic concept of critical radius?

In this chapter, we present some current ideas about these questions.

## NUCLEATION OF FRAZIL CRYSTALS

Nucleation is a general term referring to the formation of a new, embryonic phase from a parent phase. In this case, ice crystallizes from water, which is the parent phase. The fundamental thermodynamic requirement for nucleation to take place is a certain level of supercooling in the parent phase, i.e., the temperature of the water must be below the equilibrium freezing point of water; if the water is pure (no dissolved impurities) the freezing point is, by definition, 0°C at atmospheric pressure. If the water is indeed pure and contains neither dissolved impurities nor any undissolved particles such as dirt, bacteria, etc., then ice nucleation will *not* occur until an impressively large supercooling is attained. This limit is called the homogeneous nucleation supercooling, which for water is in the neighborhood of 40°C, i.e., the water must be cooled to –40°C before ice will nucleate (Mossop 1955).

Natural bodies of water are not pure; they contain both dissolved and undissolved materials. Under these conditions, the undissolved particles can act as a catalyst, whereby ice nuclei can form on these particles at supercoolings that are much smaller than the homogeneous limit. This type of nucleation is called heterogeneous nucleation. The ability of these particles to enhance nucleation is related to the geometry and chemistry of their surfaces. Perhaps the best known ice nucleating catalyst is silver iodide, which is an inorganic solid and has a heterogeneous nucleation supercooling of 3 to 4°C (Fletcher 1968). Organic particles can also be efficient ice nucleators; certain bacteria can nucleate ice at supercoolings as low as 1°C (Lindow et al. 1978). Unfortunately, natural bodies of water seldom, if ever, are supercooled by 1°C. Measurements in streams just prior to the onset of frazil ice growth indicate a much smaller supercooling, on the order of 0.1°C or less (Carstens 1966, Osterkamp et al.

1973). At this level of supercooling, there is no known catalyst that has such a low heterogeneous nucleation limit. This has led to the concept of secondary nucleation or collision breeding (Strickland-Constable 1972, Botsaris 1976) as a mechanism for the creation of frazil ice crystals.

Secondary nucleation refers to the process where tiny ice fragments (on the order of a few micrometers in size) are shed from an existing large ice crystal when it collides with a solid surface in the water or when it collides with another large ice crystal. Experiments, using both ice and salt crystals (Garabedian and Strickland-Constable 1974, Garside and Larsen 1978), have indicated that large numbers of small fragments are generated by low-energy collisions of crystals at low supercoolings. These tiny fragments then act as growth centers for new frazil ice crystals. In this way, a few seed crystals can very quickly generate first, second, third, etc., generation ice nuclei that grow into frazil ice crystals, as long as supercooling persists in the water. It is easy to see that secondary nucleation can quickly generate the number of frazil ice crystals that are often observed in laboratory and field studies (frazil ice concentrations are typically on the order of $10^6$ crystals/$m^3$ [Schaefer 1950]). The two conditions necessary for secondary nucleation are 1) turbulent motion of the water, and 2) the presence of seed ice crystals.

Sufficient turbulent motion is generated in streams and rivers where the current is greater than approximately 1.0 m/s (Carstens 1970); in lakes, surface turbulence can be created by wind and waves. With turbulence and a small degree of supercooling, frazil ice will be produced if some seed ice crystals are introduced into the water. These seed crystals can come from a number of different sources. Since frazil ice generally forms when ambient air temperatures are lower than approximately –8°C, vapor evaporating from the water surface will encounter cold air and can sublimate into ice crystals. These ice crystals will then fall down to the water surface where they are entrained by the turbulent motion of the water. Osterkamp et al. (1974) have observed this seeding mechanism in the field.

Small water droplets are also generated at the surface of turbulent water by breaking waves and bubbles bursting at the surface. These droplets are ejected into the cold air where they can readily freeze and subsequently fall back into the water to act as seed crystals (Gosink and Osterkamp 1986). Other possible sources of seed crystals are border ice, which generally forms along the banks of a river, cold dirt particles that

fall to the surface of the water and act as heterogeneous ice nucleators (termed contact nucleation [Cooper 1974]), and snow or sleet. Undoubtedly, the seeding mechanism is some combination of the above sources, depending on the meteorological conditions; however, once seeded, secondary nucleation is responsible for the prodigious volume of frazil ice that is often generated in rivers at freezeup.

## FRAZIL ICE MORPHOLOGY

Of the many different ice crystal shapes that are observed in nature, none are as elegant in their simplicity as frazil ice crystals. During growth, frazil generally evolves as thin, circular, disk-shaped crystals. Depending on the conditions under which frazil crystals grow, their maximum disk diameter is on the order of 1 or 2 mm, while their thickness varies from approximately 10 to 100 μm. This disk morphology directly results from the strong anisotropic growth rates for ice's two crystallographic directions.

When water freezes, water molecules arrange themselves into hexagonal unit cells that act as the basic building blocks for all ice crystals (Fig. 1). For our purposes, there are two principal directions of growth: along the $c$-axis, which is the axis to the unit cell, and the $a$-axis, which is perpendicular to the $c$-axis. The ice growth rates in these two directions are controlled by two very different mechanisms. Jackson (1958) and Jackson et al. (1967) have presented a general theory to characterize the roughness of a
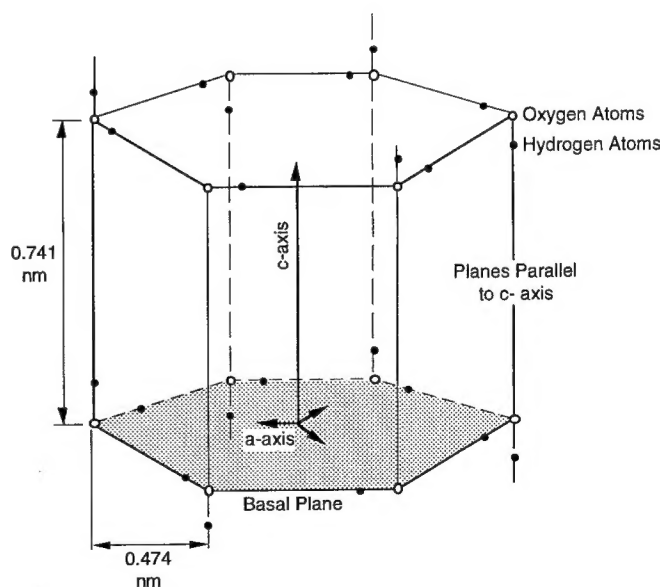


Figure 1. Shape of unit cell for hexagonal ice.

2

solid/liquid interface. They define the parameter $\alpha$ for a crystallographic plane as

$$\alpha = \frac{\varepsilon L}{R T_0} \tag{1}$$

where $\varepsilon$ = fraction of the total binding energy of an atom that can be associated with an atomic layer parallel to the face under consideration
$L$ = latent heat of fusion
$R$ = universal gas constant
$T_0$ = melting temperature of ice.

Jackson concluded that a crystal face will be smooth when $\alpha > 2$ and will be rough when $\alpha < 2$. The kinetics (i.e., the attachment of water molecules to the ice surface) for a smooth crystal is more likely to be so slow that it will control the growth rate; in this case, the crystal face will have large flat faces. Conversely, for rough crystal faces, the attachment kinetics is rapid enough that the surface grows continuously; in this case, the dissipation of latent heat from the interface limits the growth rate. Fujioka (1978) has shown that values for $\alpha$ for the a- and c-axis directions are 0.88 and 2.64 respectively. This implies that the growth in the a-axis is limited by the diffusion of latent heat, while c-axis growth is limited by some kinetic attachment mechanism.

For frazil ice crystals, the c-axis grows by the consecutive nucleation of thin monolayers spreading across the flat crystal face. For growth to occur, a stable island must be nucleated on the growing surface that quickly spreads across, covering the crystal face. The general form for c-axis growth is

$$V = \mu_1 e^{\mu_2 / \Delta T_i} \tag{2}$$

where $V$ = growth velocity
$\mu_1, \mu_2$ = constants
$\Delta T_i$ = interfacial supercooling, i.e., the difference between the interface temperature $T_i$ and the temperature in water far away from the interface $T_\infty$.

For the a-axis, the general form of growth rate is

$$V = \mu_3 \Delta T_i \tag{3}$$

where $\mu_3$ is a constant related to a heat transfer coefficient. In general, the value of $T_i$ is different for each face of the crystal. Experiments (Hillig 1958, Michaels et al. 1966) have shown that at the low levels of supercooling under which frazil crystals evolve, the growth rate in the c-axis direction is one to two orders of magnitude smaller than that in the

a-axis direction. As a result of these two different growth mechanisms, frazil crystals evolve as thin, circular disks with thickness-to-diameter aspect ratios in the range of 0.05 to 0.2 (Bukina 1963).

## STABILITY OF FRAZIL CRYSTALS

Frazil ice crystals most likely originate from the tiny ice fragments that are generated by crystal–crystal collisions. Even though there is a supply of small ice nuclei, a question remains as to whether these nuclei will grow or decay; furthermore, if nuclei grow, is there any size limit to their growth? In this section, the thermodynamics of crystal evolution in supercooled water will be briefly reviewed.

The thermodynamic concept of a critical radius is used to decide whether nuclei grow or dissolve. For any phase transition, a critical radius can be defined as the size of a nucleus that is in thermodynamic equilibrium with the surrounding parent phase. It can be shown that this equilibrium state is unstable. That is, if the size of a nucleus is less than the critical size, it will dissolve back into the parent phase; if it is larger than the critical size, it will grow (Turnbull and Fisher 1949). Note that the critical size is a thermodynamic variable just as temperature or pressure is a thermodynamic variable. For crystals in a supercooled melt, the critical size or radius $R_c$ is given by the Gibbs-Thomson equation (Dufour and Defay 1963)

$$R_c = \frac{2\gamma v_s}{L\left(\dfrac{\Delta T}{T_0}\right)} \tag{4}$$

where $\gamma$ = surface free energy of a solid/liquid interface
$v_s$ = specific volume of the solid
$L$ = specific latent heat of fusion
$T_0$ = freezing point of the pure liquid (0°C for water).

The supercooling $\Delta T$ is the difference between the equilibrium freezing point of the liquid $T_m$ and the actual temperature of the liquid $T_\infty$. For most natural bodies of water that contain some dissolved solids, $T_m$ will be slightly less than $T_0$. This freezing point depression $\Delta T_m = T_0 - T_m$ is given as

$$\Delta T_M = R T_0^2 C_0 \tag{5}$$

where $C_0$ is the molar concentration of material dissolved in the liquid (kmol dissolved material/kmol

3

liquid); eq 5 assumes that $C_o \ll 1$. If the dissolved material, e.g., salts, dissociate in solution, the expression for $\Delta T_m$ is more complicated. Osterkamp (1978) gives a thorough discussion of this point for river water and concludes that $\Delta T_m$ is on the order of 0.005°C. Equation 4 assumes that the nucleus is spherical; if the nucleus has some other shape, such as a disk, the expression for the critical radius will differ from eq 4. For example, if a frazil disk is modeled as a "stubby" cylinder (Fujioka and Serkerka 1974) then

$$R_c = \frac{\gamma\, v_s}{L\left(\dfrac{\Delta T}{T_o}\right)} .$$

(6)

If the temperature of the liquid phase is equal to the equilibrium freezing point $T_m$, then $\Delta T$ approaches zero and the critical radius becomes infinite. Physically, this implies that all nuclei, regardless of their size, will start to dissolve into the liquid phase. Thus, frazil ice crystals will only be able to survive and grow if the water temperature is less than the freezing point $T_m$.

The traditional derivation of the Gibbs-Thomson equation assumes that the presence of a crystal nucleus does not alter the thermodynamic state of the parent phase, i.e., supercooling or concentration of dissolved material. This is true if the nucleus is surrounded by an infinite volume of liquid phase. However, frazil ice crystals appear in large concentrations (on the order of $10^6/m^3$), which implies that the thermodynamic state of the water will be affected by their presence. For a sufficiently large supercooling (on the order of 0.1°C), a large fraction of frazil nuclei survive and begin to grow, since the size of the crystals is greater than the critical size (which is on the order of 0.40 µm for this level of supercooling). As each crystal grows, the ice phase rejects dissolved material to the remaining liquid phase. The concentration of dissolved material in the liquid phase slowly increases, resulting in an increase in the equilibrium freezing point depression, according to eq 5. If this change in concentration takes place at a fixed liquid temperature $T_\infty$, then the supercooling $\Delta T$, defined above, decreases. According to eq 4, the critical size therefore increases, but remains less than the physical size of the crystals. At some point, the increase in concentration of the liquid phase is enough to make the critical size equal to the physical size of the crystals. The crystals now reach a new equilibrium state that is stable.

Such increases in concentration of the liquid phase during periods of frazil growth have been measured in field studies by Osterkamp et al. (1975). Such a stability analysis was carried out (Forest 1986) for frazil crystals with a distribution in crystal thickness. The thermodynamic model predicted that the stable equilibrium radius of the frazil crystals increased with an increase in crystal thickness. The results showed that for the observed range of thickness (approximately 10 to 80 µm), the stable equilibrium radii varied from approximately 50 µm to several millimeters, depending on the supercooling. One of that work's principal conclusions was that thinner disks will quickly reach a limiting size that can be relatively small and then cease to grow. For thicker disks, the limiting size is very large, which implies that these disks are free to grow as long as there is enough supercooling to drive the growth process. This type of growth rate dispersion phenomenon, where small crystals have a much smaller average growth rate than larger crystals, has been observed previously (Cise and Randolph 1972).

To completely understand the evolution of frazil crystals, we must couple the thermodynamic stability analysis to an accurate model for predicting the growth rates of frazil crystals.

4

# CHAPTER 2

# Experimental Investigation of Frazil Ice

KATHLEEN D. WHITE AND STEVEN F. DALY

## NOMENCLATURE

$d$      pipe diameter
$f$      friction factor
$Q$      heat loss rate
$R_h$      hydraulic radius
$t_s$      time to maximum supercooling
$\bar{u}$      average velocity
$u_*$      friction velocity
$\varepsilon$      turbulent energy dissipation rate
$\kappa$      Von Karman's constant
$\nu$      kinematic viscosity

## INTRODUCTION

Laboratory experiments have been a valuable tool for developing an understanding of some aspects of the growth and evolution of frazil ice crystals. As described in Chapter 3, frazil ice can evolve through many forms in natural water bodies. In general, however, the distances are too large and the time scale too long to replicate this evolution in any laboratory setting. As a result, laboratory experiments have concentrated upon the formation phase, which is characterized by supercooled water, rapidly growing disk-shaped crystals, and the creation of new crystals by secondary nucleation.

Frazil forms over relatively compact length and time scales. In fact, the formation phase can be duplicated in a laboratory beaker, and so is amenable to laboratory study. Other laboratory experiments have examined the rise velocity of frazil disks and the interaction of frazil disks with suspended sediment. Laboratory work has also been inspired by the concept of desalination of sea water by freezing. In this context, frazil ice is viewed as an industrial product that is manufactured in bulk crystallizers.

In this chapter, we will concentrate on experiments simulating frazil ice in natural water bodies.

## FRAZIL ICE FORMATION

As Chapter 4 describes, the basic environmental parameters controlling frazil ice dynamics are the rates of heat loss, crystal seeding and turbulent en-ergy dissipation. Every frazil ice experiment has required that the investigator set these parameters and then observe the result. Unfortunately, investigators often have not been able to directly control the seeding rate, but rather have allowed the environmental conditions created in the coldroom to do it. So, seldom has the resultant seeding rate been measured.

The heat loss rate and turbulent energy dissipation rate can be determined from the description of the experimental apparatus and the experimental procedure, even if these values have not often been reported. These last two parameters, then, provide us with a straightforward and relatively easy way of comparing the various experiments (see Daly and Axelson [1989] for a more complete analysis) and it is usually possible to calculate these values as described below.

The heat loss rate $Q$ may be determined from the rate of temperature decline in the turbulent water before frazil forms. To determine the turbulent energy dissipation rate, the Reynolds number of the flow in the experiment is computed from the average velocity and a characteristic length. For pipe flow, the diameter of the pipe is the characteristic length, and for open-channel flow, the hydraulic radius is the characteristic length. The friction factor is determined from the Reynolds number of the flow using an estimated surface roughness. For pipe flow, the turbulent energy dissipation rate may be found using

$$\varepsilon = \frac{f^{3/2}\bar{u}_3}{2d} \tag{7}$$

where   $f$ = friction factor
        $\bar{u}$ = average velocity
        $d$ = pipe diameter.

For open-channel flow, the turbulent energy dissipation rate is a function of the friction velocity $u_*$, which is the product of the friction factor and the mean velocity

$$u_* = \bar{u}\left(\frac{f}{8}\right)^{1/2} . \tag{8}$$

5

The turbulent energy dissipation rate is then

$$\varepsilon = \frac{u_*^3}{\kappa R_h}\left[\ln\left(\frac{u_* R_h}{\nu_h}\right) - 1\right] \qquad (9)$$

where $\kappa$ is von Karman's constant, generally set equal to 0.4, and $R_h$ is the hydraulic radius.

Table 1 contains a summary of data from the frazil ice experiments described below, in which the water temperature record as a function of time was the primary result. Frazil ice production is generally inferred from this result, a reflection of the great difficulty in measuring the concentration or size distribution of the frazil ice crystals themselves. Figure 2 depicts the range of values for heat loss rate and turbulent energy dissipation rate found from the experimental data.

Michel (1963) carried out over 80 frazil ice growth experiments in an outdoor recirculating flume, constructed of a Plexiglas channel, 30.5 cm wide by 30.5 cm deep by 6.7 m in length, connected to a 15-cm-diameter Plexiglas pipe, although data were reported for only one test. A 20-cm-diameter, variable-speed pump with a cast iron casing circulated the water that was pumped into the flume. Many of the tests were done at night, with the air temperature ranging from –6.7 to –32°C. Water temperature was measured every 15 seconds by a differential thermometer that was accurate to ±0.0025°C.

The water temperature decline rate was reported and we calculated the heat loss rate from this. Assuming that the experiment was dominated by the turbulence immediately downstream of the pump, we calculated the turbulent energy dissipation rate for this flow area. Michel reported an average flow of 375 gal./min (0.025 m³/s), yielding a velocity in the pipe of 73 cm/s, a Reynolds number of $8.3\times10^4$ and a friction factor of 0.023. We then found the turbulent energy dissipation rate using eq 7, and we measured the time to maximum supercooling from his figure.

Carstens (1966) studied frazil ice in a recirculating oval flume, 20 cm wide by 30 cm deep by 600 cm long, located in a –10°C coldroom. The water was 20 cm deep and was circulated by a variable speed propeller. The bottom and sides of the acrylic flume were insulated, and cooling of the water was aided by a fan blowing along the straight portion of the flume. Water temperature was measured with a hand-held mercury thermometer marked to 0.01°C that was immersed from 5 to 10 cm. In a typical test, Carstens measured the water temperature decline rate and then determined the heat loss rate. For the experiments reported, the average flow velocity was 50 cm/s, yielding a Reynolds number of $1.8\times10^4$ and friction factor of 0.019. We calculated the turbulent energy dissipation rate using eq 9. Unfortunately, for several of the experiments shown in Carstens' Figure 5a, the turbulent energy dissipation rate could not be calculated because the velocity of the

**Table 1. Summary of experimental data.**

| Experimenter | Description of experiment | Test no. | $t_s$ (min) | $Q$ (J/cm³ s) | $\varepsilon$ (cm²/s¹) |
|---|---|---|---|---|---|
| Michel (1963) | Outdoor recirculating flume. | 27 | 3.3 | $1.2\times10^{-3}$ | 33 |
| Carstens (1966) | Recirculation flume in –10°C coldroom; propeller in tank in –10°C coldroom. | 6A | 4 | $1.9\times10^{-3}$ | 13 |
| | | 5A | 8 | $3.9\times10^{-4}$ | — |
| Hanley and Michel (1977) | Cylindrical tank with paddles in coldroom. Varied coldroom temperature and velocity. | –2°C | 38.1 | $0.9\times10^{-4}$ | 3 |
| | | –5°C | 21.6 | $1.9\times10^{-4}$ | 3 |
| | | –10°C | 14.7 | $3\times10^{-4}$ | 3 |
| | | –20°C | 8.1 | $7.1\times10^{-4}$ | |
| Tsang and Hanley (1985) | Warm air jacket around tank, except test C, which was in recirculating flume. Varied salinity. Seeded with shavings of ice. Average coldroom temperature –10°C. | A2(48‰) | 118.8 | $1.9\times10^{-3}$ | 2 |
| | | B1-3(23‰) | 43.6 | $2\times10^{-3}$ | 2 |
| | | B1-3(11‰) | 36.4 | $2\times10^{-3}$ | 2 |
| | | B3-4(fresh) | 18.1 | $1.9\times10^{-3}$ | 2 |
| | | C-4(ocean) | 123.9 | $1.1\times10^{-3}$ | 0.7 |
| Mueller (1978) | Supercooled water first in agitation tank in warm water. | E08 | — | — | 1375 |
| | | E09 | — | — | 4667 |
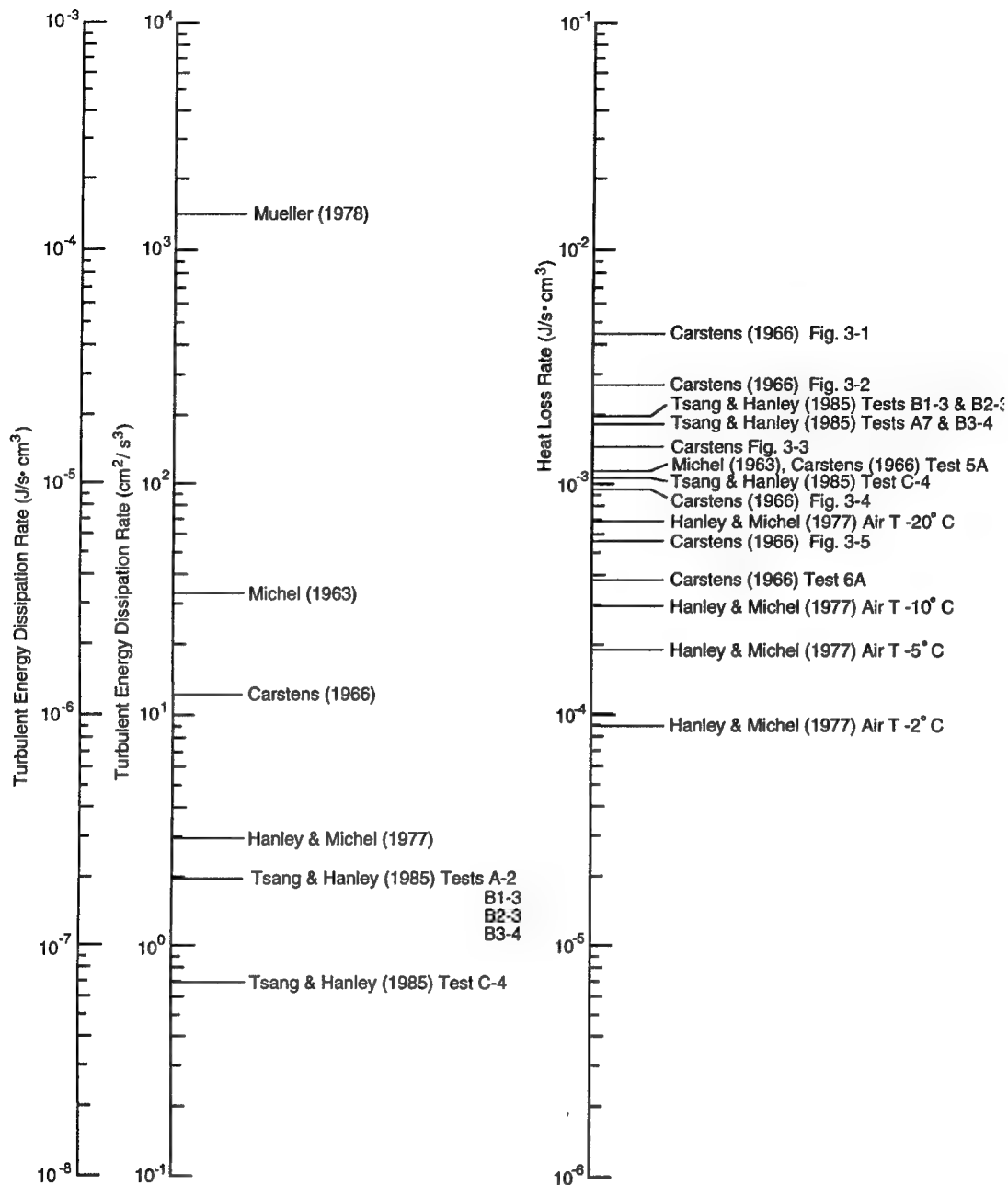
*Figure 2. Range of values for heat loss rate and turbulent energy dissipation rate from summary of the frazil ice experiments' data.*

water was not reported. However, the time to maximum supercooling could be determined from this figure and is included for comparison.

Hanley and Michel (1977) conducted frazil ice experiments in a stainless steel tank, 120 cm in diameter and 76 cm deep, at air temperatures of –2, –5, –10 and –20°C. They did not report the water depth in the tank. Paddles attached to an axis and located 25 cm above the bottom of the tank circulated the water by inducing rotational velocity. For these experiments, the coldroom temperature was set, and then the paddles started. Water temperature was measured by a thermistor placed just below the water surface. We calculated the heat loss rates from the reported water temperature decline rates. The results presented by Hanley and Michel were averaged over all velocities; the minimum velocity at which frazil growth was noted was 24 cm/s, and the

7

maximum reported velocity was 73 cm/s. Assuming a water depth in the tank of 70 cm and an average velocity of 48.5 cm/s, we calculated the Reynolds number at $8.8 \times 10^4$ and estimated the friction factor to be 0.0145. Equations 7 or 9 yielded the same turbulent energy dissipation rate. Time to maximum supercooling was not reported; total time of supercooling was reported, however, as was the time from the minimum temperature to the end of supercooling. We could estimate time to maximum supercooling by subtracting the latter from the former.

Frazil ice formation in fresh water, ocean water and artificial sea water of varying salinity was examined by Tsang and Hanley (1985). They placed a rectangular Plexiglas tank, 38 cm long by 25.5 cm wide by 15 cm deep, equipped with a stirrer at one end to provide turbulence, in a –15°C coldroom. A horizontal plate, 0.75 times the length of the tank, was placed at mid-depth to produce vertical recirculation currents, and a jacket of air, slightly above 0°C, was placed around the bottom and sides of the tank. Cooling was provided by a fan that pushed air across the surface of the water. Tsang and Hanley measured water temperature with a thermometer calibrated to 0.0001°C, with repeatability to 0.001°C. In these experiments, the water was first cooled to the previously selected temperature and then seeded either by a ball of ice or by scrapings from ice.

We picked one sample from each of their five groups of experiments for analysis here. We calculated heat loss rates for each sample as we did for Hanley and Michel. All but the group C (ocean water) experiments took place in the tank described above, with an average velocity of 15 cm/s. Water depth was not reported and we assumed it to be 15 cm. For these experiments, we calculated the Reynolds number to be $3.9 \times 10^3$, with a resulting friction factor of 0.031, and we estimated turbulent energy dissipation rates using eq 7. Group C tests took place in a recirculating flume, 15 cm wide by 13 cm deep, with a water depth of 11 cm, and average velocity of 15 cm/s. Tsang and Hanley reported the Reynolds number as $8.54 \times 10^3$. From this, we estimated the friction factor to be 0.025, and we estimated the turbulent energy dissipation rate using eq 9. Time to maximum supercooling was reported.

Mueller (1978) studied the frazil nucleation process using an agitating tank, 17.2 cm long by 12 cm wide by 20 cm deep, in a coldroom kept slightly above 0°C. The tank was surrounded by a jacket through which a coolant was circulated. Agitation was provided by a grid submerged in the tank. In these experiments, the water was supercooled to the desired degree, the coolant circulation was stopped, agitation was begun and the supercooled water seeded. Water depth ranged from 20 to 20.5 cm. He recorded the temperature using linear type thermistors that were accurate to ±0.02°C in air and ±0.002°C in water. Turbulent energy dissipation rates were reported. These experiments were not designed to allow the time to maximum supercooling to be determined, as the water was not seeded until the maximum supercooling was achieved. We report the turbulent energy dissipation rates only for comparison with the other experiments.

## OTHER ASPECTS OF FRAZIL ICE

Daly and Colbeck (1986) conducted a series of experiments designed to measure the size distribution of frazil ice crystals at four equally spaced locations along a refrigerated hydraulic flume. Several different slopes and bottom roughnesses were tested in an approximately –12°C coldroom. A crystal imaging system was used to obtain photographs of frazil crystals within a control volume at about mid-depth. Unfortunately, physical constraints imposed by the experimental conditions (e.g., flow depth) and the crystal imaging system limited measurements to the longitudinal number distribution of frazil ice crystals. Vertical number distribution could not be measured.

Ice crystal diameters determined from the photographs ranged from 35 μm to 0.5 mm, with mean aspect (diameter to thickness) ratios of 6.37, 7.45, 8.53 and 9.61 at the four measurement stations, from upstream to downstream. The number concentration of frazil ice crystals ranged from 0.17 to 0.982/cm³. Although the mean frazil crystal size and number concentration generally increased in the downstream direction, they did not increase consistently for each test. The production of anchor ice, which acted as a sink for suspended crystals, was thought to be the major cause for the variation.

Experiments examining the distribution or concentration of frazil ice in the water column have been hindered by the lack of accurate measurement techniques. In fact, in a review of frazil ice formation, Ostercamp (1978) stated that "..the most critical need is for instrumentation that can be used to measure the frazil ice concentration in a cross section of a river...". A number of researchers (e.g., Kristinsson

1970) have used changes in conductivity resulting from ice formation to estimate concentration; however, their results appear to be inconclusive. A calorimetric method of measuring frazil ice concentration currently being developed has been tested in the laboratory (Lever et al. 1992), with encouraging results.

Ettema et al. (1984) examined frazil ice nucleation and formation in a rectangular turbulence jar equipped with an oscillating grid. The water was supercooled by chiller elements containing an ethylene glycol solution at –2°C, and natural seeding was limited by keeping the room temperature above freezing. The supercooled water was artificially seeding by the addition of a small block of ice for most experiments. In some experiments, a syringe of water was withdrawn from the turbulence jar, exposed to a piece of solid ice, and then returned to the jar, presumably containing ice nuclei.

Despite the numerous difficulties typical of laboratory frazil ice experiments, the researchers were able to obtain data for calibrating their analytical model. Ettema et al. reported that the rate of frazil ice formation was directly proportional to the turbulence intensity of the water body. Frazil crystal diameters ranged between about 2 and 16 mm; the larger crystal diameters were associated with increased turbulence intensity and also with greater initial supercooling.

The rise pattern and velocity of frazil ice crystals, parameters important in frazil entrainment, transport and deposition, have been observed using frazil ice obtained in the field and in the laboratory. Gosink and Ostercamp (1983) reported on a series of tests conducted in the Chatanika River, where they collected a sample of river water in a transparent graduated cylinder and then observed the movement of the visible frazil ice crystals. Rise velocity, measured by timing the vertical displacement of the crystals, ranged from 3 to 22 mm/s. Crystal diameters, estimated using the gradations on the cylinder, ranged from 1 to 6 mm.

Wuebben (1984) used a similar method to measure rise velocities of artificial frazil ice crystals and ice crystals produced in a hydraulic flume located in a coldroom. He measured rise velocity against the vertical displacements of frazil crystals in a plastic cylinder, finding rise velocities of about 0.8 to 5.4 mm/s for estimated 0.4- to 4-mm crystal diameters.

The interaction between rising frazil ice crystals and suspended sediment was the subject of a study by Kempema et al. (1986). They did both freshwater and saline (0, 29 and 36 ppt salinity) tests; this chap-

ter discusses the freshwater tests. They used an oval recirculating flume, located in a laboratory coldroom, whose sides and bottom were insulated so that heat would be lost primarily through the surface of the water. A 4-cm thick layer of sand was placed on the bottom of the flume, where the water was then 17 cm deep. Both bed load and suspended load were observed under the range of induced velocities (42 to 70 cm/s).

Typical frazil disks, 1 to 5 mm in diameter, joined together to form roughly spherical flocs up to 80 mm in diameter. These flocs rose toward the water surface, but some touched the sand bed of the flume and remained there. In addition, sediment got trapped within the flocs, at times in quantities sufficient to "sink" them. Kempema et al. believed that sediment was trapped in the voids between the crystals, rather than being incorporated into the crystals themselves.

Suspended sediment samples were taken before frazil production began and at the point of maximum frazil production: concentrations ranged from 0.133 to 0.8 g/L before frazil production, and from 0.130 to 0.4 g/L during frazil formation. The mean decrease in suspended sediment was about 34% during frazil ice production, and the concentration of sediment contained within the frazil flocs ranged from 0.94 to 20.2 g/L.

Kempema et al. also observed the interaction between anchor ice and sediment during these experiments, reporting two mechanisms for anchor ice formation: frazil flocs that attached to objects projecting into the flow and sediment-laden frazil flocs that settled to the bottom. Flocs that settled in the lee of a sand ripple were soon incorporated into the bed structure as the bedforms migrated in an ice–sediment block. This block reappeared if the ripples migrated past the buried anchor ice. Sediment concentrations measured in anchor ice samples ranged from 4.74 to 37 g/L and from 17.6 to 42.8 g/L in combination frazil–anchor ice samples. Again, the authors believed that sediment was trapped within the voids between the crystals, rather than incorporated into the crystals.

Additional experiments using the same apparatus were reported by Kempema et al. (1993) for both freshwater and saline conditions. As before, both suspended and bed sediments were incorporated into frazil and anchor ice. Concentrations of suspended particulate matter ranged from 0.94 to 20.2 g/L with a mean of 8.59 g/L in frazil flocs and from 4.74 to 42.8 g/L with a mean of 26.7 g/L in anchor ice flocs.

## SUMMARY

Laboratory experiments have been a valuable tool for providing insight into many aspects of frazil ice formation, transport and interaction with sediment. The lack of practical and efficient ways to measure frazil ice concentrations in the laboratory or the field has been a problem. The even more desirable prospect of measuring the size distribution of frazil crystals seems a distant goal. The small size, nonspherical shape, and optical properties of frazil ice present daunting obstacles to be overcome in pursuit of this goal. However, direct and unambiguous measurements such as these are necessary for progress in the development of theoretical models of frazil ice to continue.

10

# CHAPTER 3

# Evolution of Frazil Ice in Natural Water Bodies

STEVEN F. DALY

## INTRODUCTION

One chief characteristic of the "peculiar mode of ice formation" in natural water bodies known as frazil ice is the continuous evolution of its form. The major paths of this evolution are diagrammed in Figure 3. Arguably, there are many different ways of describing this evolution, but for the sake of clarity, brevity and completeness, we will identify three general phases of frazil evolution.

The first phase is formation, characterized by supercooled water, turbulent flow, the rapid growth of disk-shaped crystals, and the creation of new crystals by secondary nucleation. The length scales of the ice associated with this stage (Fig. 4) range from several micrometers to perhaps a few millimeters. This stage usually lasts for a relatively short time during very cold periods when the heat transfer from open water surface is large.

The second phase is transformation and transport. This phase follows the first in time, and results from the rapid production of the first phase. It is characterized by water more or less at the equilibrium temperature, and frazil in the form of flocs, anchor ice and floes. The length scales of the ice associated with this stage (Fig. 4) range from several millimeters to several meters. The frazil is largely mov-

ing under the influence of the river or stream, generally at the surface. This ice may travel long distances and move for many days. After cold nights, it is typical to see slush, formed of frazil flocs, moving along at the water surface of northern rivers and streams. This slush may eventually form large moving floes.

The third phase is characterized by stationary, floating ice covers that may be quite large and last for the entire winter season. These ice covers are formed by a variety of mechanisms, depending on the form of the frazil ice when it arrives at the stationary ice cover and the hydraulic conditions at the cover's leading edge. These floating covers may raise stages and cause flooding, cause increases in the channel head losses that can disrupt power production, and interfere with navigation.

To focus our discussion, we can further subdivide the three phases discussed above into six process categories (Fig. 3). Each category is distinguished by one or two distinct forms of frazil ice and one or two dominating processes. The progression of the categories in general follows the known evolution of frazil ice. We can outline each category as follows.

In the formation phase there are two categories. Seeding describes the introduction of ice crystals from outside the water body that starts the forma-



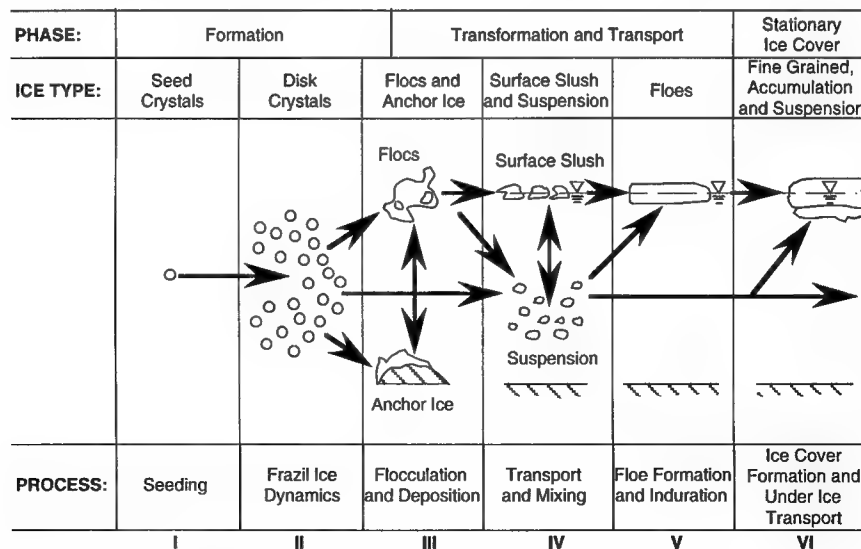| PHASE: | Formation | | Transformation and Transport | | | Stationary Ice Cover |
|---|---|---|---|---|---|---|
| ICE TYPE: | Seed Crystals | Disk Crystals | Flocs and Anchor Ice | Surface Slush and Suspension | Floes | Fine Grained, Accumulation and Suspension |
| PROCESS: | Seeding | Frazil Ice Dynamics | Flocculation and Deposition | Transport and Mixing | Floe Formation and Induration | Ice Cover Formation and Under Ice Transport |
| | I | II | III | IV | V | VI |

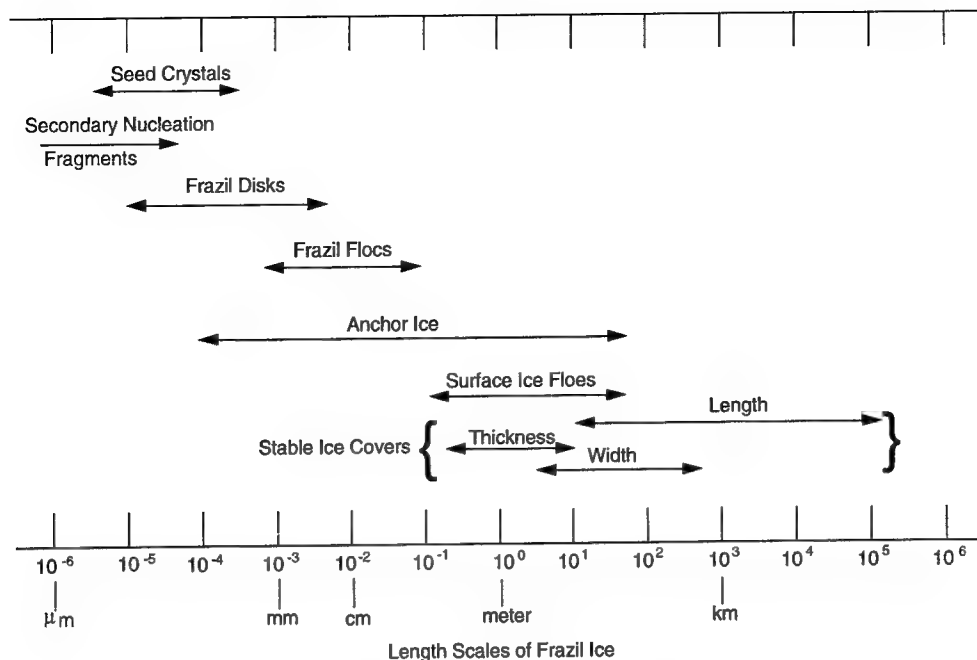Figure 3. Evolution of frazil ice in natural water bodies.

*Figure 4. Length scales of frazil ice.*

tion of frazil ice. Frazil ice dynamics describes the interaction of seeding, secondary nucleation and crystal growth. It is during this stage that disks appear, each being a separate crystal. Disk crystals are the unique form of frazil ice and the form by which it is chiefly known. These disks are formed in supercooled, turbulent water. A complete discussion of the physics and dynamics of this stage can be found in Chapters 1 and 4.

In the transformation and transport phase, frazil ice displays a marked tendency to aggregate into larger and larger masses. At this time, we cannot determine the aggregation rate, or even if the progression to larger sizes will happen at all. In general, the progression goes at a rate determined by the turbulent intensity of the flow, but very high levels of turbulence will keep the larger forms of frazil from occurring. This means that the particular evolutionary pathway followed by the frazil in its progression to larger aggradations will be unique for each water body. As a result, it is quite difficult to generalize the transformation and transport stage of frazil evolution. The three categories that occur in this stage—flocculation and deposition, transport and mixing, and floe formation and induration—describe the processes through which the initial disk crystals are transformed into larger and larger ice masses. The length scales associated with these forms can become quite large (Fig. 4).

The small disk crystals of frazil ice, which start at the size of millimeters, can eventually form very large river ice covers with lengths of many kilometers and thicknesses of many meters (the stationary ice cover, phase six).

We will now discuss each of the categories and the various forms of frazil that define each.

## SEEDING

For a long time, the origin of frazil ice under natural conditions was debated. Spontaneous nucleation of ice, either heterogeneously or homogeneously, was thought responsible for the ultimate origin of frazil. All available data indicate that spontaneous nucleation of ice is not possible in natural water bodies; therefore, seed crystals are necessary (Daly 1984). Unfortunately, there is very little quantitative information available on either the sizes of the seed crystals or the seeding rates. Osterkamp (1977) reports that hexagonal plate ice crystals, ranging from 60 to 350 $\mu$m, were observed in the air above a supercooled Alaskan stream. Their concentrations ranged from 6 to $6 \times 10^4$ crystals/m$^3$. It is possible to estimate a surface seeding rate from the concentration of crystals suspended in the air $C_A$ as

$$I_s = C_A u_f \tag{1}$$

where $u_f$ is the terminal fall velocity of the ice crystals. The terminal fall velocities of the largest and smallest ice crystal are estimated as 17 and 5 cm/s, respectively (Pruppacher and Klett 1978), yielding a

12

seeding rate per unit surface area of $3 \times 10^{-5}$ to 1.0 crystals/cm² s. For a discussion of other mechanisms for producing seed crystals see Chapter 1.

## FRAZIL ICE DYNAMICS— DISK CRYSTALS

We know from observations that the dominant shape of ice crystals that grow at the supercooling levels found in turbulent water bodies is a flat disk. Virtually all field observations of frazil ice note that the crystals are disk shaped. It has been reported that ice crystals in the shape of six-pointed stars, hexagonal plates or spheres, and small pieces of dendritic ice all evolve into the disk shape in natural water bodies.

Disk-shaped crystals have been studied in the laboratory by Kumai and Itagaki (1953), Arakawa (1954) and Williamson and Chalmers (1966). Arakawa created disk crystals by first growing dendritic ice crystals on the bottom of a container containing slightly supercooled water. He then scratched the crystals with the tip of a fine needle. Spherical ice particles with a diameter of about $10^{-2}$ mm rose towards the surface; two flat spots formed on the spherical particles' surface as they floated up. Further growth was lateral; the particles became disks. The crystals grew into disks with diameters of 0.5 to 3 mm and with diameter-to-thickness ratios of 5:1 to 100:1. Once the disks grew to a certain size they took on a notched look, with many notch-shaped growths at their perimeters.

The disk shape of the ice crystal is morphologically instable. In natural water bodies, this instability is observed as scalloped edges, dendritic

growths, irregular protuberances, etc., on the perimeter of the crystals. Experiments have shown that the disk shape always becomes unstable if the supercooling is large or if the diameter of the crystal is large. Instability is perhaps the mechanism that limits the maximum disk radius size. The entire reason for the instability of the disk shape is not known, although it has been the subject of several investigations (Williamson and Chalmers 1966, Fujioka and Sekerka 1974). Williamson and Chalmers concluded that the instability of the disk shape depends on heat flow into the liquid, not crystallography. This conclusion seems correct, as the diameter at which the crystal becomes unstable varies between experiments.

Disk-shaped frazil ice crystals have been observed under three contexts: in natural water bodies, in laboratory experiments and in research into desalination by freezing. The difficulties in measuring frazil size or concentration have limited the number of measurements made.

Estimates of the range of frazil crystal concentrations in natural rivers is from about 10,000 to 1 million crystals/m³ (Schaefer 1950, Osterkamp and Gosink 1982). Measurements in a laboratory flume (Daly and Colbeck 1986) indicated concentrations ranging from $1.80 \times 10^5$ to $9.82 \times 10^5$ crystals/m³.

The sizes of crystals have been measured in the range of 0.05 mm to several millimeters (Daly and Colbeck 1986). The aspect ratio of the crystals is shown in Figure 5. The observations of Margolis (1969) on frazil ice grown during desalination by freezing indicate that the thickness of the frazil disk is $(0.68 \pm 0.17)R$, where $R$ is the major radius of the disk. Smith and Sarofin (1979) report that the maximum diameter is approximately 1.6 mm for disk crystals produced in turbulent crystallizers.

## FLOCCULATION AND DEPOSITION

### Frazil flocs

The flocculation of frazil ice is not well understood, although sintering is one mechanism used to explain it. Sintering apparently results from the tendency of crystals to minimize their surface energy. Martin (1981) stated that for disks of thickness on the order of 1–10 μm, the time for bonds to form is fast, perhaps $10^{-2}$ seconds. Mercier (1984), in his simulations, assumed that turbulent shear and differential rising were the two mechanisms causing collisions of crystals for sintering.
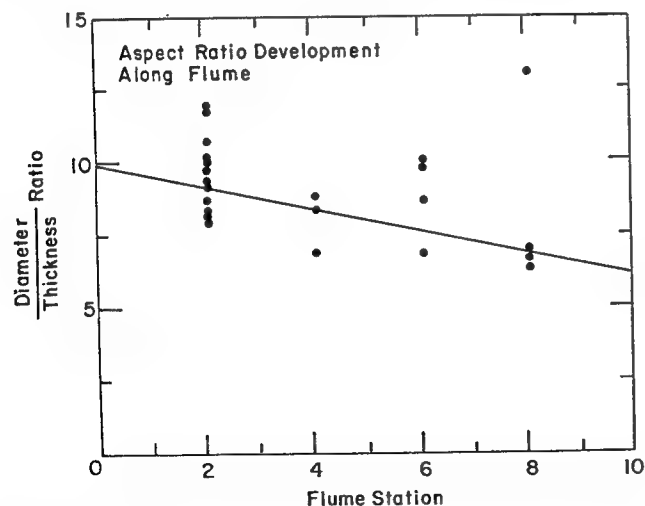


Figure 5. Size distribution of the major crystal diameters measured in a laboratory flume (from Daly and Colbeck 1986).

Descriptions of flocs in streams (Osterkamp and Gosink 1982) and observations by this author suggest that flocs are formed initially by a few to several hundred frazil disks. The bonds within newly formed flocs are initially very weak, and they will often collapse when removed from the water. Large flocs, called frazil pebbles, were described by Chacho et al. (1986) as ranging in length from less than 5 to greater than 150 mm. Grains composing the frazil pebbles do not possess a preferred c-axis orientation, but appear to show alignment related to grain size and shape. This may imply that these pebbles are not formed by collisions caused by turbulent shear, which would presumably result in randomly oriented grains, but probably result from differential rising or a depositional mechanism, such as might take place during the formation of anchor ice. The round shape of the pebbles may result from mechanical abrasion, indicative of the long distance that they may have traveled on the Tanana River before they were observed, or represent the equilibrium form of flocs that have traveled long distances under water.

### Anchor ice

There has been little quantitative study (Marcotte and Robert 1986) of anchor ice, which is formed initially by the deposition of suspended frazil crystals. Once deposited, the heat transfer rate from the anchor ice is much greater than that for the suspended frazil. The importance of anchor ice as a sink of suspended crystals and as a source of latent heat in an overall stream crystal balance or heat balance will be inversely proportional to the hydraulic radius of the stream. Anchor ice may be the dominant form of frazil produced in shallow streams.

## TRANSPORT AND MIXING

### Frazil slush

Frazil slush is the collection of frazil flocs and individual frazil crystals on the water surface in a distinct layer. The mechanical properties of the highly porous frazil slush are not known. A sample of frazil slush lifted from the water will quickly drain, revealing a characteristic white appearance. On the surface it has a marked tendency to form a "structure" of independent, individual clumps, that eventually become floes.

How this structure arises is, at present, unknown. It may well arise "spontaneously" as numerical simulations of cohensionless, inelastic particles suggest (Hopkins and Lange 1991), or it may

result from the buffeting of the slush by surface eddies. The degree to which the formation of a structure is aided by the mechanical interlocking of the rough frazil flocs is also unknown. In any case, the initial clumps that are formed can be broken up upon reaching a highly turbulent portion of river.

Tsang (1988) reported 15% concentrations of ice in the surface layer at the Cachine Rapids of the St. Lawrence River. Matousek (1981) cited densities of frazil slush from 300 to 640 kg/m$^3$, density and porosity being linearly dependent on the mean air temperature.

### Suspension

The form of the frazil ice that is in suspension can vary so widely that it is difficult to adequately describe it. The form will chiefly depend on the frazil's past history. Close to the point of formation, more disk crystals will be found in the suspension; far from the point of formation, there will be more flocs. Another consideration is the relative time that the ice has spent on the surface as compared to being in the depth of the flow. If the frazil has traveled on the surface and then been resuspended (by passing into a zone of high turbulence, for example), a very high proportion of flocs could be expected.

Arden and Wigle (1972) observed frazil ice in suspension on the Niagara River, where frazil ice was largely in the form of disks. They viewed the suspension with an underwater lamp at night, giving "the viewer the impression that he is looking at a driving snowstorm, as seen through the headlight beams of a moving automobile at night."

There are very few measurements of the concentration of frazil ice in suspension. One profile, measured by Tsang (1986) using a device that inferred the concentration of frazil based on the electrical conductivity of the water, gave values in the range of 0 to 0.03%.

### Determination of vertical transport

To adequately discuss the vertical mixing of frazil ice requires that the size distribution and form of the frazil crystals be well known, that the buoyancy of the frazil can be determined, that the turbulence of the water flow field be well described, that the heat transfer rate from the water surface be known, and that the evolution in form of the frazil in response to these influences can be estimated. Unfortunately, at present, we know very little of the above. Because of this, investigators have concentrated on specific questions, such as: What is the buoyant rise velocity of frazil disks

and frazil flocs? Under what conditions of flow and heat loss can a distinct surface layer of slush be expected to form? What is the concentration of frazil ice in suspension?

Matousek (1984) determined the flow conditions under which a distinct surface layer could be expected by comparing the buoyant rise velocity of frazil disks and the mean magnitude of the turbulent velocity fluctuations in the vertical direction. If the rise velocity exceeded this mean magnitude, then a surface layer should form. Empirical correlations were used to determine both the rise velocity and the vertical velocity fluctuations.

Gosink and Osterkamp (1983) compared the buoyant and mixing time scales to determine "well mixed vs. layered" flow. If the buoyant time scale (defined by the time required for a disk to rise through the entire depth) was less than the time required for the frazil disk to diffuse downward through the entire depth, then they expected a distinct surface layer to form. Interestingly, the ratio of the time scales is independent of the flow depth, and depends only on the mean flow velocity, the channel roughness and the rise velocity of the frazil. They assumed the rise velocity to be 0.01 m/s, which is appropriate, based on their analysis, for disks 2.5 mm in diameter, with a thickness-to-diameter ratio of 1:10.

Tsang (1988) compared the kinetic energy available for mixing and the increase in potential energy resulting from suspension of the frazil ice in the flow. From this he derived a "distribution equation," which, when solved numerically, provided the vertical concentration distribution of the frazil ice, including a distinct surface layer, if present.

Lal (1989) and Gunaratna (1989) developed "two layer" models, with one layer corresponding to the distinct surface layer and the other to the suspended frazil. Essentially, the ice exchange between the layers was determined by one parameter whose value was found through model calibration.

Ho (1990) determined the vertical diffusion of the frazil through the water depth by solving the Fickian diffusion equation. Several empirically determined coefficients were required in this approach.

Liou and Ferrick (1992) developed a model in which the net upward migration of frazil disks attributable to buoyancy was opposed by intermittent mixing induced by large energy-containing eddies. A surface renewal model was used to describe the effects of large eddy mixing. They supposed that a critical surface layer thickness was necessary for the surface to develop structure. In general, they found that the heat loss rate from the water surface, the surface renewal frequency, and the critical surface layer thickness determined whether the frazil evolved towards a well-mixed equilibrium state or a layered state.

## FLOE FORMATION

How floes form from frazil ice flocs is probably one of the least well described processes in the evolution of frazil ice. As mentioned previously, frazil slush at the water surface shows a marked tendency to clump together. The initial clumps, if they remain on the surface long enough, freeze together and form pans, or small floes. These pans often grind against one another, become roughly circular and gain upturned edges, and then are known as pancake ice. The pans can also stick together and form much larger floes, which attain sizes comparable to the river's width.

Pans are always much smaller than the stream width, and as a result, their form is essentially independent of the stream geometry. Larger floes, on the other hand, result from changes in the stream surface velocities that tend to concentrate pans at specific points along the stream channel. The form of these large floes then is strongly controlled by the particular flow conditions of the streams.

The formation of floes of all sizes is governed by two separate but intertwined processes: the increase in floe area and floe induration. The increase in floe area reflects the accumulation of frazil ice into a single, moving unit. Floe induration describes the increase in floe strength because of exposure to the cold air. Immediately after their formation, floes are quite porous and have little strength. Eventually, they may become more or less solid ice as the interstitial water freezes. The relation among the floe porosity, size and strength is not known at the present. The only measurements of floe strength are those by White (in prep.), who estimated in-situ floe strength by suspending instrumented rods in a mountain stream during a period when frazil ice floes were present. She observed three types of interactions between the rods and the ice floes: a "crushing-type" interaction, in which the rod left an indentation track in the floe; a liquid-like interaction, where the floes "flowed around the rod" and resumed their original shape with no discernible tracks; and solid-impact interactions, where the floes bounced off the rod. She was able to draw only qualitative inferences between the type of interaction and the air temperature, travel distance and appearance of the floes.

15

Osterkamp and Gosink (1982) described floe formation in interior Alaskan streams in detail. They identified five mechanisms that can produce floes from smaller frazil pans: 1) contact, penetration and bonding of the frazil pans; 2) compaction and drag cutoff*; 3) compaction and convergent flow with cutoff by impact of incoming pans; 4) extrusive flow and drag cutoff; and 5) agglomeration with cutoff controlled primarily by river curvature. Extrusive flow and drag cutoff produced very large floes on the Yukon River, with maximum dimensions exceeding 1 km.

## ICE COVER FORMATION AND UNDER-ICE TRANSPORT

The formation of river ice covers by frazil ice proceeds by a number of processes (Ashton 1986, Michel 1971, Osterkamp and Gosink 1982). The particular process at any given point is determined largely by the form of the frazil, the hydraulic conditions of the flow, and the heat transfer rate from the water surface. The cover can be considered initiated when the frazil ice first stops because of an ice or hydraulic control structure, because of the growth of surface ice in a slow moving reach, or because the moving frazil ice has "arched" across the open water. The arching of floes has been the subject of some investigation, but arching of frazil slush has received much less attention, although its occurrence in the field has been reported (Osterkamp and Gosink 1982). That frazil slush can arch implies that it has the ability to transmit shear stresses, but the effective viscosity of slush and its other material properties are not known.

A major issue for hydraulic engineers studying the formation of ice covers is determining the conditions for stability of the frazil ice arriving at the cover's leading upstream edge. The arriving ice is said to be stable if it retains orientation and shape at the time that it stops at the leading edge.

The form of frazil ice arriving at the upstream end of an ice cover plays a major role in determining if and how the frazil will be incorporated into it. Frazil ice that is largely in suspension will pass under the cover and deposit on the underside at some point downstream. Frazil slush may be incorpo-

rated into the ice cover at the surface if the flow velocity is low, may "pack" at higher velocities, or may be carried under the cover at still higher velocities. Floes may be "stable" (that is, they do not underturn) at the leading edge of the ice cover if the velocities are low, underturn and remain at the leading edge at higher velocities, and be carried under the ice cover at still higher velocities. Determining the range of hydraulic conditions at which each of these behaviors will occur has been one of the major directions of river ice research (for overviews, see for example, Michel [1978] or Ashton [1986]).

Frazil ice that is transported under an ice cover often deposits on the underside, and there is a long history of researchers considering this frazil ice deposition to be analogous to that of sediment (Pariset and Hausser 1961, etc.). How closely this analogy should be drawn is not clear; for example, many of the bed forms found in rivers transporting sediment, such as dunes, antidunes, ripples, etc., have not been reported on the underside of river ice covers transporting frazil. (It must be noted, however, that ripples have been observed to form in solid ice covers. This results from the turbulent flow beneath the cover and the associated heat transfer [Ashton 1986], not frazil transport.) The one form that has been observed, which can grow to spectacular depths, is called a "hanging dam" (Michel et al. 1981, Beltaos and Dean 1981, Hopper et al. 1981, Shen et al. 1984, Michel 1990), but this form has no recognized analogy in sediment transport.

In any case, applications of concepts from sediment transport have not proven especially useful in predicting the under-ice deposition of frazil—other than the relatively simple and straightforward concept of a "critical velocity criterion" to determine the limiting thickness of frazil deposition (Tesaker 1975, Michel and Drouin 1975, Shen et al. 1984, Michel 1984, Sun and Shen 1988). Unfortunately, the value of this critical velocity has been found to vary from about 0.9 m/s at the beginning of the winter to about 0.5 m/s at the end (Michel et al. 1981) at one location in Canada, and to vary from 0.4 to 1.2 m/s from reach to reach in the Yellow River in China (Sun and Shen 1988). Undoubtedly, the value of this critical velocity is influenced by the form of the frazil, the distance it has traveled under the ice cover, the degree of supercooling of the river and perhaps other factors.

The response of frazil slush on arriving at the leading edge of an ice cover has been described in several works of B. Michel (1991, 1986, 1984), in which frontal progression and packing are distinguished and analyzed through the use of momen-

---

* Cutoff is the process whereby distinct floes are separated from a large mass of compacted frazil ice. Drag cutoff refers to separation that occurs when the fluid drag acting on the ice exceeds the tensile strength of the compacted ice mass.

tum, energy and mass flux balances at the leading edge. The stability of floes arriving at the leading edge has most recently been analyzed by Daly and Axelson (1990) and McGilvary and Coutermarsh (1992).

## SUMMARY

The evolution of frazil in rivers and stream is influenced by the structure and growth kinetics of frazil ice crystals, the turbulent intensity of the flow, the surface heat loss rate to the atmosphere, the plan form of the river, the existence of hydraulic and ice control structures, and many other factors. In broad outline, the evolutionary pathway of frazil is well known, but little of it can be quantitatively described. At present, efforts to control or modify this evolution must rely on empirical criteria that have been obtained through experience and long observation.

# CHAPTER 4

# Frazil Ice Dynamics

STEVEN F. DALY

## NOMENCLATURE

| | |
|---|---|
| $B$ | birth function |
| $C$ | heat capacity of fluid |
| $C_i$ | heat capacity of ice |
| $C_T$ | fluid impurity concentration |
| $D$ | death function |
| $E_{rb}$ | energy created by crystal–boundary collisions |
| $E(r_1,r_2)$ | energy created by collisions of crystals of size $r_1$ and $r_2$ |
| $\dot{E}_t$ | rate of energy transfer by collision |
| $F_1$ | number of particles generated per unit of collision energy |
| $F_2$ | fraction of particles surviving to become crystals |
| $g$ | gravity |
| $g'$ | reduced gravity |
| $G$ | crystal growth rate |
| $h$ | heat transfer coefficient |
| $k$ | heat conductivity of fluid |
| $K_v$ | crystal shape factor |
| $L$ | mean latent heat of fusion of ice |
| $m^*$ | nondimensional crystal size |
| $m(r)$ | mass of crystal of size $r$ |
| $n$ | size distribution function |
| $N$ | total number of crystals per unit volume |
| $\dot{N}_I$ | rate of introduction of new crystals |
| $\dot{N}_T$ | total secondary nucleation |
| $Nu$ | Nusselt number |
| $Nu_T$ | turbulent Nusselt number |
| $Nu_o$ | Nusselt number for a particle in a stationary fluid |
| $Pe$ | Pèclet number |
| $Pr$ | Prandtl number |
| $q_{rb}$ | frequency of collisions between crystals and boundary |
| $q(r_1,r_2)$ | frequency of collisions between crystals of size $r_1$ and $r_2$ |
| $Q^*$ | net heat transfer |
| $r$ | major linear dimension of frazil crystals |
| $r_f$ | face dimension of disk |
| $R$ | region of phase space |
| $R_c$ | collision radius |
| $Re$ | Reynolds number |
| $R_h$ | hydraulic radius |
| $S_N$ | $(F_1)(F_2)$ |

| | |
|---|---|
| $t$ | time |
| $T_f$ | temperature of fluid |
| $u'$ | turbulent fluctuation of velocity |
| $U_{rb}$ | relative velocity of crystal and boundary |
| $v(r_1,r_2)$ | relative velocity of crystals of size $r_1$ and $r_2$ |
| $\vec{V}_e(R,t)$ | external phase space convective velocity |
| $\vec{V}_f$ | fluid velocity |
| $\vec{V}_i(R,t)$ | internal phase space convective velocity |
| $\vec{V}$ | particle phase space velocity |
| $\vec{V}(R,t)$ | phase space velocity |
| $\alpha$ | thermal diffusivity |
| $\alpha_T$ | turbulent intensity |
| $\delta(r-r_c)$ | Dirac delta function |
| $\psi$ | collision efficiency |
| $\varepsilon$ | turbulent dissipation rate |
| $\eta$ | dissipation length scale |
| $\theta$ | bulk supercooling |
| $\nu$ | fluid kinematic viscosity |
| $\rho_f$ | density of water |
| $\hat{\rho}_f$ | mass concentration of water in mixture |
| $\hat{\rho}_i$ | mass concentration of ice in mixture |
| $\rho_i$ | density of ice |
| $\ell_m$ | length scale of maximum eddy size |

## INTRODUCTION

In this chapter, we will discuss the development of a physically based quantitative model that describes the dynamic evolution of the frazil crystal size distribution function during the first stage of frazil evolution in natural water bodies. Two equations serve as the basis for the model: the crystal number continuity equation and the heat balance for a differential volume. The use of only two equations simplifies the presentation but is not meant to suggest any limitation; conservation of impurities (such as salt), for example, could be added (see Chapter 5). The crystal growth rate and secondary nucleation rate are the major parameters that appear in these equations. Expressions for both are derived. We will see that there are three basic environmental parameters: 1) the heat loss rate and 2) the crystal seeding rate, which appear directly in the basic equations, and 3) the turbulent energy dissipation rate, which influences both the crystal growth rate

and the rate of secondary nucleation. One material property, the number of crystals produced per unit of collision energy, directly controls the rate of secondary nucleation.

## BASIC EQUATIONS

### Crystal number continuity equation

The crystal distribution will be described in a space termed the crystal phase space or, more generally, the particle phase space. Particle phase space is defined by the least number of independent coordinates that provides a complete and useful description of the properties of the crystal distribution. It is convenient, if somewhat arbitrary, to divide particle phase space into two subregions defined by external coordinates and internal coordinates. The external coordinates describe the spatial distribution of the crystals. Internal coordinates refer to properties attached to each individual crystal, which quantitatively measure its state, and are independent of its position.

To begin, we will consider a crystal distribution function $n(R,t)$. This function is defined over a region $R$ of the particle phase space consisting of the three spatial dimensions (the external coordinates) plus any number of internal property coordinates. In all further cases the internal coordinates will be restricted to one, which will correspond to a major linear dimension $r$ of the ice crystals. The function $n(R,t)$ is defined as the population density of crystals in the region $R$. At a time $t$ the number $dN$ of crystals in an incremental region $dR$ of the particle phase space is given by

$$dN = ndR \tag{11}$$

and the total number of crystals in a region $R$ at time $t$ is

$$N(t) = \int_R ndR \cdot \tag{12}$$

It may be necessary to deal with the sudden appearance (birth) or disappearance (death) of crystals per unit region in the particle phase space. The net appearance in an incremental region $dR$ at a time would be

$$(B\text{–}D)dR \tag{13}$$

where $B(R,t)$ and $D(R,t)$ represent birth and death functions at a point in the phase space.

The population balance of crystals in some fixed region $R$, which moves convectively with the particle phase space velocity $\vec{V}$, can be defined as

$$\frac{d}{dt}\int_R ndR = \int (B-D)dR \ . \tag{14}$$

Expanding the first term using Leibnitz's rule, noting that the region $R$ was arbitrary, and that only a single internal coordinate $r$ is considered, where $G(r,t)$ is the convective velocity along $r$ or simply the growth rate of the ice crystal, we then see that

$$\frac{\partial n}{\partial t} + \frac{\partial}{\partial r}(Gn) + D - B + \nabla\left(\vec{V}_e n\right) = 0 \tag{15}$$

where $\vec{V}_e$ is the external phase space convective velocity.

This is the number continuity equation in general form. Further extensions can be made by considering the diffusion of crystals, and the rise velocity of the crystals.

### Heat balance

The general expression for the heat balance of the frazil-ice–water system will be developed strictly for frazil crystals suspended in fresh water.

Consider a differential volume in which $\hat{\rho}_f$ is the mass concentration of water (grams of water per cubic centimeter of mixture), $\hat{\rho}_i$ is the mass concentration of ice and the temperature of the water is $T_f$. It is assumed that, to good approximation

$$\hat{\rho}_f + \hat{\rho}_i \cong \hat{\rho}_f \cong \rho_f$$

A second assumption is then

$$C_i\hat{\rho}_i / C\rho_f \ll 1$$

where $C$ is the heat capacity of water and $C_i$ is the heat capacity of ice.

Additionally, heat conduction can be neglected and heat capacities and the latent heat can be considered constant because of the small variation in temperature. Therefore, based on the above assumptions, the heat balance for a mixture of frazil and water can be written

$$\frac{\partial T_f}{\partial t} + \nabla\left(\hat{V}_f T_f\right) =$$

$$\frac{L}{C\rho_f}\left[\frac{\partial}{\partial t}\hat{\rho}_i + \nabla\left(\hat{V}_e\,\hat{\rho}_i\right)\right] + \frac{Q^*}{C\rho_f} \tag{16}$$

20

where $\hat{V}_f$ = convective velocity of the fluid
$Q^*$ = net heat transfer from the mixture volume
$L$ = latent heat of fusion of the ice at the equilibrium temperature of the mixture.

## Parameters in the basic equations

The two basic equations are those for the crystal number continuity (eq 15), and the heat balance (eq 16). The various parameters that appear in these two equations will now be discussed.

1. $G$—Along the $a$-axis of frazil ice disk, it is assumed that $G$ is effectively determined by the heat transfer rate. Thus, in general

$$G = \frac{h(r,\varepsilon)}{\rho_i L}\theta$$

where $h$, the heat transfer coefficient, is a function of the crystal size $r$ and the level of turbulence $\varepsilon$, and $\theta$ is the supercooling of the mixture.

2. $D$—The death function can be set to zero for all sizes of crystals. This is equivalent to assuming that there is no large-scale breakage of the crystals.

3. $B$—The birth function is determined by the rate of the sudden appearance of new crystals. New crystals can appear as a result of spontaneous nucleation, secondary nucleation and the introduction of crystals; however, spontaneous nucleation is not possible under frazil-forming conditions. Therefore, $B$ will be determined by the rate at which new crystals are introduced and the rate of secondary nucleation.

Let $\dot{N}_T$ be the rate of secondary nucleation. $\dot{N}_T$ is a function of the crystal size distribution $n$, the turbulence dissipation rate $\varepsilon$, the supercooling of the mixture $\theta$ and perhaps other parameters. Let $\dot{N}_I$ be the rate at which new crystals are introduced. We assume that new crystals are created and introduced at a size equal to the critical radius of the crystals $r_c$. Thus

$$B = \left[\dot{N}_I(\theta,n,\varepsilon) + \dot{N}_I\right]\delta(r - r_c)$$

where $\delta(r-r_c)$ is the Dirac delta function.

4. $\hat{\rho}_i$ —The mass of ice per unit volume of mixture can conveniently be determined using the moment equation

$$\hat{\rho}_i = \rho_i K_v \int n(r)dr$$

where $K_v$ is a crystal shape function ($K_v = 4\pi/3$ for the sphere, 1 for a cube).

5. $Q^*$—This is determined by the environment of the water body of interest and, in particular, the meteorological and hydraulic conditions.

6. $\vec{V}_e, \vec{V}_f$—The convective velocity of the ice crystals and the fluid will generally be very similar. The action of buoyancy and inertial forces on the ice crystals may cause the ice crystal velocity to differ from the fluid velocity if these forces become large compared to the fluid drag force.

Substituting the above expressions into eq 15 and 16 gives us

$$\frac{\partial n}{\partial t} + \frac{\theta}{\rho_i L}\frac{\partial}{\partial r}(hn) + \nabla\left(\vec{V}_e n\right)$$
$$= \left(\dot{N}_T + \dot{N}_I\right)\delta(r - r_c) \tag{17a}$$

$$\frac{\partial \theta}{\partial t} + \nabla\left(\vec{V}_f \theta\right) = \frac{L\rho_i K_v}{C\rho_f}\left[\frac{\partial}{\partial t}\int_0^\infty r^3 n\,dr\right.$$
$$\left. + \nabla\left(\vec{V}_e \int_0^\infty r^3 n\,dr\right)\right] + \frac{Q^*}{C\rho_f} \tag{17b}$$

where  $n$ = $n(x,y,z,r,t)$
$\theta$ = $\theta(x,y,z,t)$
$h$ = $h(r,e)$
$\vec{V}_e$ = $\vec{V}_e(x,y,z,r,t)$
$\dot{N}_T$ = $\dot{N}_T(\theta,\varepsilon,n)$
$\vec{V}_f$ = $\vec{V}_f(x,y,z,t)$
$Q^*$ = $Q^*(x,y,z,t)$.

Writing the equations in this form emphasizes the dynamic way in which they interact. To determine $r$ and $n$ uniquely, both equations must be solved simultaneously, and the boundary conditions and initial conditions of $r$ and $n$ must be known. Difficulties arise because $\theta$ and $n$ are dimensionally incompatible.

## ICE CRYSTAL GROWTH RATES

### Intrinsic kinetic growth rate

The mechanisms that determine the rate at which an ice crystal can grow are the transport of water molecules to the crystal surface (for ice grown in pure water this is not a consideration), their incorporation into the crystal surface and the transport of latent heat away from the surface. The incorporation

21

of molecules is controlled by the crystallization or interface kinetics of ice, and the heat transfer reflects the particular physical situation of the system under consideration.

The interface kinetics of ice has been studied both theoretically and experimentally. As noted in Chapter 1, ice has two principal growth directions: $a$-axis and $c$-axis. The interface kinetics of each growth direction appears to be different. Growth in the $c$-axis probably proceeds by surface nucleation for perfect crystals and by a dislocation mechanism for damaged crystals. The interface kinetics of $a$-axis growth has not been completely defined; the mechanism is probably that of continuous growth. However, it appears that the kinetics is very fast and that for practical purposes the growth rate of the $a$-axis is totally controlled by the rate at which heat is transported away from the interface. Growth along the $c$-axis is much slower than that along the $a$-axis for all sizes of crystals. This implies that $c$-axis growth is controlled by the intrinsic kinetics. The $c$-axis growth rate does not appear in the number continuity equation. The latent heat released by growth along the $c$-axis may contribute somewhat to the overall heat balance; however, it may be that the latent heat released by $c$-axis growth is effectively negligible. Therefore, only the growth along the $a$-axis will be considered.

### Heat transfer from ice crystals suspended in turbulent water

In this section expressions for the rate of heat transfer from suspended ice crystals will be formulated. To determine the transfer rate, it is necessary to describe the ambient velocity distributions of the fluid about the crystal. Frazil is created and develops only in water that is turbulent. Rivers and channels are inherently turbulent because of the instability of their bulk currents, and wind can make large water bodies turbulent. Frazil is also created in crystallizers in which the water is made turbulent by impellers, turbines or other means. To describe the velocity distribution of the water surrounding the crystals requires knowledge of the properties and characteristics of turbulence.

Turbulence can be visualized as numerous interacting eddies of all possible scales. The very largest eddies originate directly from the instabilities of the mean bulk flow. The scale and orientation of these largest eddies are imposed by the geometry of the flow situation. Energy is extracted from the large eddies through the inertial interaction of these eddies with smaller eddies. The energy cascade is not affected by the fluid viscosity until the smallest scales are reached, where this energy is dissipated by the

viscosity. The dissipation rate must equal the rate at which energy is supplied to the small-scale eddies. The dissipation rate $\varepsilon$ and the fluid dynamic viscosity $\nu$ form a length scale such that

$$\eta \sim \left( \nu^3 / \varepsilon \right)^{1/4} \tag{18}$$

where $\eta$ is the dissipation length scale or the Kolmogorov scale.

If the crystal size is small relative to the Kolmogorov length scale, it is in the dissipative regime. In the dissipative regime the fluid eddies are strongly dampened and dissipated by the fluid viscosity. In effect, the crystal is smaller than the smallest scales of the turbulent eddies. It does not experience the turbulence as interacting eddies but rather as a fluid motion that varies linearly with position.

If the crystal size is large relative to the Kolmogorov length scale, it is in the inertial regime. The ambient velocity can be characterized in many different ways, each corresponding to a different eddy size. It seems reasonable to assume, following Wadia (1974), that the predominant shear that the particle will experience will be produced by eddies closest to the particle that are of the same size as the particle. Eddies that are significantly larger than the particle will entrain both the particle and the fluid around it. Very small eddies relative to the particle size may enhance the overall transport by some mechanism of renewal of the boundary layer surrounding the particles, but eddies of a size comparable to the size of the particle will cause the most significant gradients near the crystal surface.

The small-scale motion, smaller than the size of the crystal, may enhance the heat transport from the crystal by penetrating the boundary layer around the crystal. It is difficult to quantify this process but this enhancement has been successfully (although empirically) accounted for by correlation with the turbulent intensity $\alpha_T$ of the fluid. $\alpha_T$ is defined as

$$\alpha_T = \sqrt{u_f'^2 / \overline{V}} \tag{19}$$

where $\sqrt{u'^2}$ is the rms value of the velocity deviation from the mean velocity $\overline{V}_f$.

A method of determining the Nusselt number that provides an intuitively easier means of seeing the relative value of the actual heat transfer coefficient is as follows. Let $Nu_T$ be the turbulent Nusselt number defined as
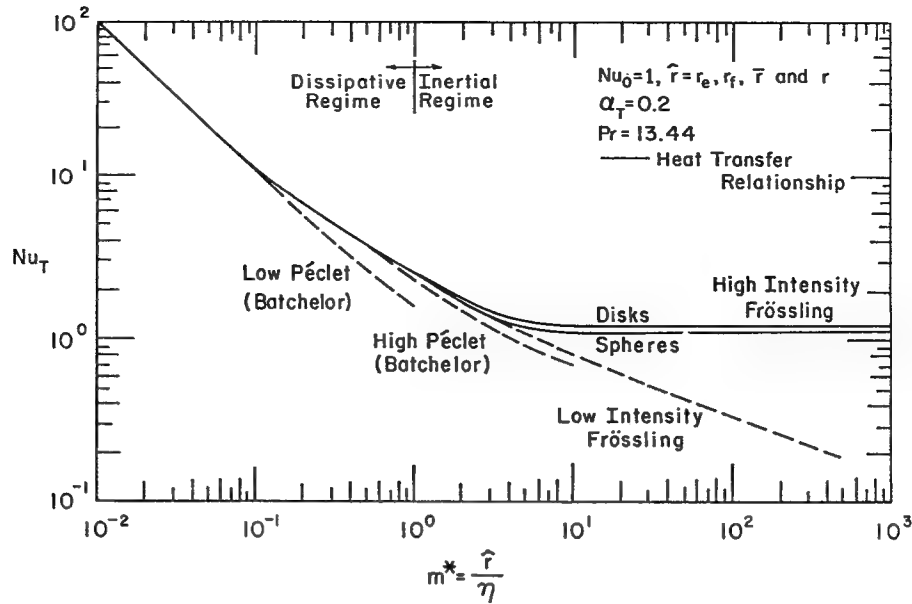
22

*Figure 6. Nusselt number relationships.*

$$Nu_T = \frac{h\eta}{k} = \frac{h}{k}\left(\frac{v^3}{\varepsilon}\right)^{1/4}$$

Let $m^* = r/\eta$. The heat transfer relationships are then as follows:

For $m^* < 1/(Pr)^{1/2}$

$$Nu_T = (1/m^*) + 0.17\,Pr^{1/2}. \qquad (20a)$$

For $1/(Pr)^{1/2} < m^* < \approx 10$

$$Nu_T = [(1/m^*) + 0.55\,(Pr/m^*)^{1/3}]. \qquad (20b)$$

For $m^* > 1$, with a low intensity $\alpha_T m^{*4/3} < 1000$

$$Nu_T = \left[(1/m^*) + 0.70\,\alpha_T^{0.035}\,(Pr/m)^{1/3}\right]. \qquad (20c)$$

For $m^* > 1$, with a high intensity $\alpha_T m^{*4/3} > 1000$

$$Nu_T = (1/m^*) + 0.70\,\alpha_T^{0.25}\,Pr^{1/3} \qquad (20d)$$

These Nusselt number relationships are shown in Figure 6.

**Secondary nucleation**

The processes that govern the rates of secondary nucleation are poorly understood. However, a partial modeling of the kinetics of secondary nucleation is possible based on the work of Evans et al. (1974a, b), who demonstrated that for ice the production rate of potential nuclei of new crystals and their removal from the parent crystals could be uncoupled. The most widely accepted source of the potential nuclei is surface irregularities that are sheared from the surface of the parent crystals (microattrition). Two general mechanisms of removal of the nuclei from the surface of the parent crystals have been suggested: collisions of the crystals with hard surfaces (including other crystals) and fluid shear. If the rate of secondary nucleation is limited by the production rate of potential nuclei, increases in the number of collisions of an individual crystal will not increase the production of new crystals. If the rate of secondary nucleation is removal-limited, however, the parent crystals will produce the same number of new nuclei each collision, independent of the crystal's time history. From their experimental work, Evans et al. (1974a,b) concluded that the secondary nucleation of ice was limited by the rate at which potential nuclei were removed from the crystal surface. Therefore, it was possible to determine the overall nucleation rate $\dot{N}_i$, with two or more mechanisms of removal, as the linear sum of the actual nucleation rate attributable to each mechanism of removal ($\dot{N}_i$)

$$\dot{N}_T = \dot{N}_1 + \dot{N}_2 + \dots \dot{N}_i \qquad (21)$$

The nucleation rate of each mechanism of collision can be expressed as the product of three functions (Botsaris 1976)

$$\dot{N}_T = (\dot{E}_t)(F_1)(F_2) \qquad (22)$$

23

where $\dot{E}_t$ = rate of energy transfer to crystals by collision

$F_1$ = number of particles generated per unit of collision energy

$F_2$ = fraction of particles surviving to become nuclei.

At this time the values of $F_1$ and $F_2$ must be determined empirically. Therefore, to simplify matters, let $F_1$ and $F_2$ be combined and eq 22 be rewritten as

$$\dot{N}_t = \dot{E}_t S_N \tag{23}$$

where $S_N = (F_1)(F_2)$.

We expect that $S_N$ is a function of all the parameters that govern the surface morphology and the crystal growth, including supercooling $q$, impurity concentrations $C_T$, turbulence level $\varepsilon$, etc. The total nucleation rate can be expressed as

$$\dot{N}_T = S_N\left(\theta, \varepsilon, C_T, \text{ etc.}\right)\left(\dot{E}_{t1} + E_{t2} + \dot{E}_{t3} \ldots\right). \tag{24}$$

## SUMMARY

In this chapter a physically based quantitative model of frazil ice was described. Two equations serve as the basis of the model: the crystal number continuity equation and the heat balance for a differential volume. One focus of the chapter has been describing in detail two of the major parameters that appear in this model: the crystal growth rate and the secondary nucleation rate. Both involve complex interaction of the crystals with the fluid turbulence. Three basic environmental parameters and one material property control the evolution of the crystal size distribution function. These environmental parameters are the heat loss rate, the turbulent energy dissipation rate of the fluid, and the crystal seeding rate; the material property is the number of crystals produced per unit of collision energy. A tremendous amount of literature describes the first two of these parameters, and virtually none the third; a modest literature is available on secondary nucleation, with very little describing ice.

The importance of a quantitative model such as described here is that it allows predictions to be made that can be tested in laboratory experiments. By controlling or measuring the environmental parameters in experiments, knowledge of the resulting size distributions would allow estimates of the growth rate and secondary nucleation rate to be tested. Unfortunately, the measurement of the crystal size distribution is quite difficult, even in the laboratory. However, such tests would advance our fundamental understanding of frazil ice evolution, and the efficient solution of practical problems could not be far behind.

# CHAPTER 5

# Numerical Simulation of Frazil Ice

ANDERS OMSTEDT

## NOMENCLATURE

| | |
|---|---|
| $C_f$ | frazil ice concentration, volume fraction |
| $C_g$ | grease ice concentration, volume fraction |
| $C_\mu, C_{1_\varepsilon}, C_{2_\varepsilon}, C_{3_\varepsilon}$ | constants in the turbulence model |
| $c_p$ | specific heat of sea water |
| $d$ | diameter |
| $d_e$ | crystal thickness |
| $d_f$ | crystal face diameter |
| $d_s$ | diameter for a sphere |
| $E$ | coefficient for collision efficiency |
| $F_c(t)$ | mass exchange or seeding |
| $F_N(t)$ | net heat loss at the air/water interface |
| $f$ | Coriolis' parameter |
| $G_{C_f}, G_{Coll}, G_s, G_H$ | source–sink terms attributable to ice formation |
| $k$ | turbulent kinetic energy |
| $k_w$ | thermal conductivity of water |
| $L$ | latent heat of ice |
| $Nu$ | Nusselt number |
| $P$ | pressure |
| $P_b$ | source–sink term attributable to buoyancy production |
| $P_s$ | source–sink term attributable to shear production |
| $q$ | heat transfer between ice and water |
| $S$ | water salinity |
| $T$ | water temperature |
| $T_f$ | freezing temperature |
| $T_m$ | temperature of maximum density |
| $T_{min}$ | maximum supercooling |
| $T_n$ | supercooling at seeding |
| $t$ | time |
| $t_c$ | characteristic time |
| $U$ | mean velocity in $x$-direction |
| $u_r$ | collision velocity |
| $V$ | mean velocity in $y$-direction |
| $\overline{V}$ | mean velocity vector |
| $x$ | horizontal coordinate, positive in east direction |
| $y$ | horizontal coordinate, positive in north direction |
| $z$ | vertical coordinate, positive upwards |
| $\varepsilon$ | dissipation of turbulent kinetic energy |
| $\nu$ | kinematic viscosity |
| $\nu_T$ | kinematic turbulent viscosity |
| $\rho_f$ | frazil ice density |
| $\rho_g$ | grease ice density |
| $\rho_M$ | mixture density |
| $\rho_w$ | water density |
| $\sigma_{C_f}$ | turbulent Schmidt number for $C_f$ |
| $\sigma_{C_g}$ | turbulent Schmidt number for $C_g$ |
| $\sigma_k$ | turbulent Prandtl–Schmidt number for $k$ |
| $\sigma_S$ | turbulent Schmidt number for $S$ |
| $\sigma_H$ | turbulent Prandtl number for heat |
| $\sigma_\varepsilon$ | turbulent Prandtl–Schmidt number for $\varepsilon$ |

## INTRODUCTION

### Scope of the chapter

The purpose of this chapter is to review the numerical modeling of frazil ice in water bodies. The recent developments in the field of computational fluid mechanics have made it possible to include advanced turbulence models in environmental flow simulations. This, together with increased knowledge about the thermal regime during freezing and frazil ice dynamics, provides us with a good starting point for numerical simulations of frazil ice.

To begin with we should, however, recall that models do not give any new information. Instead they provide us with a logical framework in which we can add our knowledge and test our ideas—as such a "laboratory," in which we do not get cold and wet.

### Physical processes to be considered

Initially, ice forms in turbulent waters by the introduction of ice crystals from the atmosphere, which become suspended in the supercooled water (see Fig. 7). As ice formation proceeds, the suspended ice crystals increase in size and number, stick to the bottom or rise towards the surface, flocculate and form clusters with high porosity. In the ocean, salt is also rejected from the ice crystals. The physical processes to be considered therefore include cooling, turbulent mixing, mass exchange with the air and the water, and ice growth, multipli-
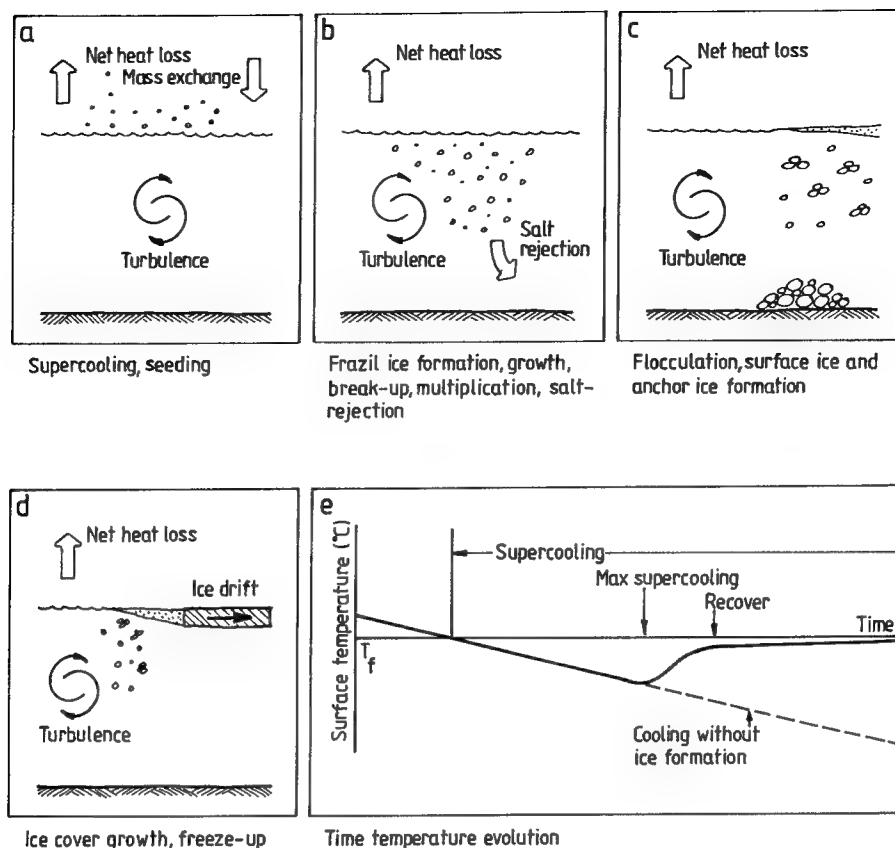
25

Figure 7. Process of initial ice formation in turbulent water bodies.

cation and flocculation. The frazil ice evolution is thus a complex interaction among fluid flow, heat and mass transfer.

## GUIDANCE AND SIMPLIFYING ASSUMPTIONS

### Turbulence

Frazil ice forming under turbulent conditions implies that we need to consider a relevant boundary layer flow. In oceans, a turbulent Ekman flow, and in rivers, a turbulent channel flow are the most basic boundary layers. These boundary layers will therefore be discussed here.

Different approaches to solving the boundary layer equations are available, yet they all start from conservation equations for mean properties, e.g., mean temperature and mean momentum. The different approaches adopted can basically be divided into integral models and closure models of turbulence. The integral or mixed layer models are based upon the observation that the mean properties are often time-dependent but constant in a vertical direction within a mixed layer. Verti-

cal integration of the conservation equations then gives ordinary differential equations for the bulk properties. The closure models of turbulence involve the Reynolds averaging of the conservation equations and the derivation of the average products from different assumptions about the mixing processes.

The approach adopted in this chapter is to choose a closure model of turbulence with the closure level according to a two-equation model of turbulence. This kind of model has been tested with success for many different kinds of flows. The model therefore owes its strength to its generality (Rodi 1980, 1987).

### Mass exchange and morphology

Several field observations report that the frazil ice formation begins at supercoolings on the order of 0.01–0.1°C. The initial nucleation of frazil ice in nature is therefore believed to be caused by seeding or mass exchange with the atmosphere (Osterkamp 1977). In laboratory studies, we can also observe that, for temperatures close to freezing, the amount of supercooling before frazil ice starts to form is al-

most completely determined by the seeding time (Hanley and Tsang 1984). Field and laboratory observations also indicate that the initial crystals grow into small disks and that further ice production is associated with crystal multiplication. These observations guide us to include mass exchange with the atmosphere and to regard the ice as small crystals suspended in the water.

## Gravity

Another obvious observation is that the ice crystals are lighter than the water. Turbulent kinetic energy is therefore needed to suspend the crystals. The conversion of turbulent kinetic energy into potential energy has thus to be considered in the modeling work. This is a key feature for the mixing of the upper layers of the ocean, and also when studying suspended sediment in a bottom boundary layer. It is also believed to be important for the frazil ice formation.

## Salt rejection

During frazil ice formation, the temperatures are close to the temperature of freezing, and no salt can therefore crystallize. Instead, all salt is probably rejected from the interior of the crystal out to the crystal surface, where it is mixed with surrounding water. In fact, freezing can work as an effective method to separate salt from water. This implies that we could assume that almost pure ice crystals are formed during frazil ice formation and that nearly all salinity is rejected out into the surrounding water body.

## Flocculation

As cooling proceeds, frazil flocs (grease ice) are observed on the water surface. They have then overcome the turbulent mixing through gravity. This observation indicates that large crystals or flocs of crystals may become so large that mixing is insufficient. Flocculation may therefore work as the main mechanism for surface ice formation in turbulent waters.

## REVIEW OF THE LITERATURE

There are a large number of models on mixed layer dynamics in the ocean and in rivers; however, very few are directed to the numerical simulation of frazil ice.

In the ocean, Danard et al. (1983) presented a model for initial sea ice formation. Frazil ice forma-tion was, however, not considered in their approach; only cooling was considered.

Bauer and Martin (1983) illustrated how we could treat ice formation in small leads. In their model they considered the pile-up of frazil flocs to result from wind and waves. Also considered was how the ice cover advanced upwind until the entire lead was ice covered. Pease (1987) examined ice production in a Bering Sea polynya, and illustrated that the polynya width is ascribable to a balance between frazil ice production and ice advection. Bulk transfer coefficients for heat and momentum over leads and polynyas were presented by Andreas and Murphy (1986).

Omstedt and Svensson (1984) developed a frazil ice model for a turbulent Ekman flow. The basic idea was that frazil ice should be described by a boundary layer approach, in which buoyancy effects from frazil ice should be included. Omstedt (1985a) verified the model against laboratory data and extended it to the upper layers of the ocean (Omstedt 1985b).

Mellor et al. (1986) considered the turbulent boundary layer under drifting sea ice and the response to melting and freezing. In the freezing simulation, a small amount of supercooling was modeled throughout the mixed layer, and the authors suggested that this could be associated with the formation of frazil ice. Steele et al. (1989) introduced a new scheme for the simulation of the molecular sublayers. In the case of freezing, the amount of supercooling was increased because of the large difference between molecular heat and salt diffusion.

Freysteinsson (1970) discussed how frazil ice in a river can be calculated on the basis of the thermal heat balance and a regression analysis for the amount of open water. Ginsburg (1979) reviewed methods of forecasting frazil ice in rivers. The review illustrated how conditions for frazil ice formation could be presented in a diagram for a specific reservoir. Abramenkov (1980) introduced a flocculation equation for the formation of frazil ice in rivers.

Starosolszky (1981) reported on a survey conducted by the World Meteorological Organization (WMO) on frazil ice forecasts. A system of ice forecasting was also outlined.

Matousek (1981) presented a mathematical model for frazil ice in a river with steady flow. The model was based on the thermal balance of a river and semi-empirical relations for the ice. Conditions for frazil ice formation were formulated by Matousek (1984) on the basis of a balance between rise velocity and turbulent mixing (see also Gosink and Osterkamp 1983).

Daly (1984) reviewed the frazil ice dynamics and

outlined the basic equation for the crystal number continuity.

Marcotte and Robert (1986) presented a first attempt to model anchor ice in rivers.

Nyberg (1986, 1987) and Sahlberg (1990) applied the model of Omstedt (1985b) to rivers. In the applications, frazil ice and frazil-floc dynamics were considered as well as the melting of frazil ice. Some of the results were earlier reviewed by Omstedt (1986).

In recent work, Svensson and Omstedt (1994) presented a model of frazil ice dynamics where the crystal number continuity equation was solved for a well-mixed jar. The following processes were studied: initial seeding, secondary nucleation, gravitational removal, growth ascribable to cooling of the water volume and flocculation–breakup.

In the next section the basic equations are introduced. In the *Details of Calculations* section, the numerical scheme used by the present author and his colleagues is briefly discussed. Results from the numerical simulations of frazil ice in the laboratory, ocean and river flows are reviewed in the section that follows. Then, in the *Forecasts* section, that problem is addressed. Finally, a *Discussion* is given.

## MATHEMATICAL FORMULATION

The main part of the water in nature is ocean water. In fact, fresh water constitutes only 2.7% of the global water budget (Ashton 1986). In the salinity range from fresh water to ocean water, we also have brackish waters, which are often close to the coast and therefore in areas with a high degree of human activity. For example, the Baltic Sea and adjacent seas (the world's largest estuary) have salinities ranging from almost zero to levels found typically in the ocean.

Salinity, temperature and pressure influence several properties in the water. For processes close to the surface, pressure effects can often be neglected. Pressure effects will therefore not be dealt with in this chapter. SI units are used for all variables except temperature, for which degrees Celsius are used.

### Properties of water and ice

The freezing temperature $T_f$ as well as the temperature of maximum density $T_m$ are functions of salinity $S$

$$T_f = -0.0575\,S + 0.00171\,S^{1.5} - 0.000215\,S^2 \quad (22)$$

$$T_m = 3.982 - 0.2229\,S \quad (23)$$

where $S$ is expressed in parts-per-thousand. See Appendix 3 in Gill (1982), and Caldwell (1978).

From the equations we can see that saline water is freezing at lower temperatures compared with fresh water. In oceans the freezing temperature also becomes greater than the temperature of maximum density, a feature of great importance in homogeneous, stratified seas where cooling is always associated with convection. This is in contrast to fresh or brackish water bodies, in which cooling is associated with the formation of a stable, stratified surface layer. The surface water density ($\rho_w$) is a function of temperature and salinity. If nonlinear effects are neglected, the equation reads

$$\rho_w \cong 999.84 + 0.068\,T + S\,(0.82 - 0.004\,T). \quad (24)$$

See Appendix 3 in Gill (1982) for the complete equation.

The importance of temperature and salinity in density calculations depends on the studied water body. For example, in estuaries, which are often highly stratified because of a brackish surface layer on top of a more saline layer, the salinity almost completely controls the stratification.

The thermal conductivity ($k_w$) is slightly dependent on temperature and salinity. According to Caldwell (1974) the equation reads

$$k_w = 0.5719\,(1 + A_1 T - A_2 T^2 - A_4 S) \quad (25)$$

where $A_1 = 0.003$, $A_2 = 1.025 \times 10^{-5}$ and $A_4 = 0.00029$.

The specific heat is a function of salinity and temperature. Again, disregarding the nonlinear terms, the specific heat for fresh water reads approximately

$$c_p(S=0) \cong 4217.4 - 3.7\,T. \quad (26)$$

The corresponding equation for sea water reads

$$c_p \cong c_p(S=0) + S(-7.6 + 0.1\,T). \quad (27)$$

See Appendix 3 in Gill (1982) for the complete equation.

The latent heat of fusion ($L_f$) is a complex function of temperature and salinity (see Yen 1981 or Weeks and Ackley 1982). In the case of frazil ice formation, all salt is probably rejected out from the crystal, and pure ice crystals are formed.

### Heat equation

The starting point for the heat budget is the conservation equation for heat energy. The derivation followed is analogous to the derivation of the Rey-

nolds equation; thus, heat is decomposed into a mean and a fluctuating part, and the equation is then time-averaged. If horizontal mixing is not dealt with, the equation reads

$$\frac{d}{dt}\rho_w c_p T = \frac{\partial}{\partial z}\left(\frac{v_T}{\sigma_H}\frac{\partial}{\partial z}\rho_w c_p T\right) + G_H \qquad (28)$$

where  $z$ = vertical space coordinate positive upwards
$t$ = time coordinate
$v_T$ = kinematic eddy viscosity
$\sigma_H$ = Prandtl number
$G_H$ = source–sink term associated with freezing–melting.

The left-hand side denotes the total change of heat, thus

$$\frac{d}{dt}\rho_w c_p T = \frac{\partial}{\partial t}\rho_w c_p T + \text{div}\left(\overline{V}\rho_w c_p T\right).$$

The boundary conditions for the heat equation have to consider the energy budget above the surface and the sediment heat from the bottom. As frazil forms in open water areas, large amounts of ice can be produced. This is in contrast to columnar ice growth, where the ice itself drastically reduces the heat exchange to the atmosphere.

Before solving eq 28, we can notice some basic balances. If the equation is vertically integrated and advection is not dealt with, the steady-state solution is a balance between the net heat loss and the release of latent heat associated with freezing. If advection becomes important, other basic balances may exist. Advection may, for example, balance the net heat loss and inhibit ice formation.

### Salt equation

From a conservation point of view, introducing mean and fluctuating salinities and time averaging gives

$$\frac{dS}{dt} = \frac{\partial}{\partial z}\left(\frac{v_T}{\sigma_S}\frac{\partial S}{\partial z}\right) + G_S \qquad (29)$$

where  $\sigma_S$  is the Schmidt number for salinity and  $G_S$  the source–sink term associated with freezing–melting.

The boundary conditions have to consider evaporation and precipitation. Melting and freezing enter the equation through the source–sink term. Again we can notice some basic balances, the most obvious being a balance between the ice formation and the local salinity increase.

### Frazil ice equation

The derivation of the frazil ice equation follows the same path as above (see also Omstedt 1985b). The equation reads

$$\frac{dC_f}{dt} = \frac{\partial}{\partial z}\left(\frac{v_T}{\sigma_{C_f}}\frac{\partial C_f}{\partial z}\right) + G_{C_f} - G_{Coll} \qquad (30)$$

where  $C_f$ = mean volume fraction of frazil ice
$\sigma_{C_f}$ = Schmidt number for frazil ice
$G_{C_f}$ = source–sink term associated with freezing–melting
$G_{Coll}$ = sink term associated with flocculation.

The frazil ice rise velocity is included on the left side of eq 30.

The boundary conditions at the air/water interface have to consider the mass exchange with the atmosphere. At the water/bottom interface, anchor ice may have to be considered.

Three basic balances can be noticed. Firstly, there is a balance between turbulent mixing and rise velocity that controls whether surface ice may form or whether the crystals are kept in suspension. Secondly, there is a balance between frazil ice formation and flocculation. When large amounts of crystals are suspended, the probability that the crystals will flocculate increases, and thus only a certain amount of individual crystals can be kept in suspension. Thirdly, there is a balance between frazil ice formation and anchor ice production. Almost all crystals may in some situations form ice on the bottom, and no surface ice will then form.

### Frazil-floc equation

The approach adopted by the present author is to introduce a second ice equation to simulate the frazil-flocs (grease ice). The derivation follows the same ideas as above

$$\frac{dC_g}{dt} = \frac{\partial}{\partial z}\left(\frac{v_T}{\sigma_{C_g}}\frac{\partial C_g}{\partial z}\right) + G_{Coll} \qquad (31)$$

where  $C_g$ = mean volume fraction of frazil-flocs
$\sigma_{C_g}$ = Schmidt number for frazil-flocs
$G_{Coll}$ = source–sink term associated with flocculation.

The frazil-floc rise velocity is included on the left side of eq 31.

29

Table 2. Source–sink terms associated with frazil ice and frazil-floc formation.

| Morphology | $G_H[W\,m^{-3}]$ | $G_C[s^{-1}]$ | $G_S[s^{-1}]$ | $G_{Coll}[s^{-1}]$ |
|---|---|---|---|---|
| Spherical crystals | $\dfrac{6qC_f}{d_s}$ | $\dfrac{6qC_f}{d_s\rho_f L}$ | $\dfrac{6qSC_f}{d_s\rho_w L}$ | $\dfrac{3Eu_r C_f^2}{2d_s}$ |
| Plate crystals | $\dfrac{4qC_f}{d_f}$ | $\dfrac{4qC_f}{d_f\rho_f L}$ | $\dfrac{4qSC_f}{d_f\rho_w L}$ | $\dfrac{Eu_r C_f^2}{d_e}$ |

The boundary condition is that there are no fluxes at the vertical boundaries.

We can see from the equation that frazil-flocs are assumed to form only because of flocculation and not through thermal processes. Some basic aspects of eq 31 can be noticed. Firstly, because of larger aggregates of ice, the rise velocity will rapidly overcome the turbulent mixing, and the ice will float up to the surface. Secondly, the formation of surface ice may become an outcome of the balance between ice production and advection (see also Bauer and Martin 1983).

In the present approach, we thus distinguish between two ice regimes, frazil ice and frazil-flocs. Another way of looking at the equations is to say that we distinguish between small crystals, which are formed because of thermal processes, and larger crystals, which are aggregates of the smaller crystals.

A summary of the different source–sink terms associated with ice formation is given in Table 2, where the heat transfer $q$ and the collision velocity $u_r$ are according to

$$q = \frac{Nu\,k_w}{d_e}\left(T_i - T\right)$$

$$u_r = \left(\frac{1}{15}\right)^{1/2}\left(\frac{\varepsilon}{\nu}\right)^{1/2} d_f$$

where  $Nu$ = Nusselt number
$T_i$ = ice temperature
$k_w$ = thermal conductivity of water
$\nu$ = kinematic viscosity
$\varepsilon$ = dissipation of turbulent kinetic energy
$d_e$ = ice crystal thickness
$d_f$ = ice crystal face diameter.

For the derivation of the source–sink terms, see Omstedt (1985b).

It should be noticed that the source–sink terms associated with frazil ice formation are linearly dependent on the frazil ice concentration, while the source–sink terms associated with flocculation are proportional to the square of the frazil ice concentration. The underlying assumption is that the collision velocity is independent of the frazil ice concentration.

## Mixture density equation

The frazil ice problem is a typical two-phase flow, where ice is one phase and water the other. In the field of computational fluid mechanics, it is today possible to solve multiphase flows. However, the present author believes that a diffusion or mixture formulation may hold for many applications. From the mixture formulation, the distribution of the dispersed phase is calculated from scalar equations, such as eq 30 and 31.

To include the concentrations in the mixed layer dynamics, we introduce a mixture density equation according to

$$\rho_M = \rho_w + (\rho_f - \rho_w)C_f + (\rho_g - \rho_w)C_g \qquad (32)$$

where $\rho_f$ is the frazil ice density and $\rho_g$ the frazil-flocs' density.

When a mixture density is introduced in the dynamics, an increased frazil formation will be associated with the formation of a stably stratified surface layer. The turbulent mixing thus has to work against gravity and turbulent kinetic energy is therefore transformed to potential energy.

## Boundary layer equations

Starting from the Navier-Stokes equation, introducing mean and fluctuating velocities and time-averaging the equation, we derive the Reynolds equation. In this section we shall reduce the equation and only outline two basic boundary layers, namely the turbulent Ekman flow and the turbulent channel flow.

The Ekman boundary layer equations read

$$\frac{\partial U}{\partial t} = \frac{\partial}{\partial z}\left(\nu_T \frac{\partial U}{\partial z}\right) + fV \qquad (33)$$

$$\frac{\partial U}{\partial t} = \frac{\partial}{\partial z}\left(\nu_T \frac{\partial V}{\partial z}\right) - fU \qquad (34)$$

where $U$ and $V$ are mean velocities in horizontal direction and $f$ is Coriolis' parameter.

30

The channel boundary equation reads

$$\frac{\partial U}{\partial t} = \frac{\partial}{\partial z}\left(\nu_T \frac{\partial U}{\partial z}\right) - \frac{1}{\rho_w}\frac{\partial P}{\partial x} \qquad (35)$$

where $\partial P/\partial x$ is the horizontal pressure gradient.

The boundary condition for the air/water interface is related to the wind stress, and at the water/bottom interface, the velocities are set equal to zero.

The fundamental balances are between the vertical shear, associated with the wind stress, and the earth rotation or the vertical shear, associated with the bottom friction, and the horizontal pressure differences.

## Turbulence model

Several turbulence models exist and, as stated earlier, we have chosen to use a two-equation model of turbulence, with one equation for the turbulent kinetic energy $k$ and another for the dissipation rate of turbulent kinetic energy $\varepsilon$ (see Svensson 1979 or Rodi 1987). The turbulent mixing processes are assumed to be caused by current shear and convection caused by cooling and salt rejection. The turbulent mixing processes are described by vertical exchange coefficients. The introduction of exchange coefficients and gradient laws excludes counter-gradient fluxes. Breaking waves and Langmuir circulation are not dealt with. The equations read

**Table 3. Constants in the turbulence model.**

| Constant | Value |
|---|---|
| $C_\mu$ | 0.09 |
| $C_{1\varepsilon}$ | 1.44 |
| $C_{2\varepsilon}$ | 1.92 |
| $C_{3\varepsilon}$ | 0.8 |
| $\sigma_k$ | 1.4 |
| $\sigma_e$ | 1.4 |

$$\frac{dk}{dt} = \frac{\partial}{\partial z}\left(\frac{\nu_T}{\sigma_k}\frac{\partial k}{\partial z}\right) + P_s + P_b - \varepsilon \qquad (36)$$

$$\frac{d\varepsilon}{dt} = \frac{\partial}{\partial z}\left(\frac{\nu_T}{\sigma_e}\frac{\partial \varepsilon}{\partial z}\right)$$
$$+ \frac{\varepsilon}{k}\left(C_{1_e} P_s + C_{3_e} P_b - C_{2_e}\varepsilon\right) \qquad (37)$$

$$P_s = \nu_T\left(\left(\frac{\partial U}{\partial z}\right)^2 + \left(\frac{\partial V}{\partial z}\right)^2\right) \qquad (38)$$

$$P_b = \frac{\nu_T g}{\rho_o}\left(\frac{\partial \rho_w}{\partial z} + \frac{\rho_f - \rho_w}{\sigma_{C_f}}\frac{\partial C_f}{\partial z}\right.$$
$$\left. + \frac{\rho_g - \rho_w}{\sigma_{C_g}}\frac{\partial C_g}{\partial z}\right) \qquad (39)$$

$$\nu_T = C_\mu \frac{k^2}{\varepsilon} \qquad (40)$$

where $P_s$ is the production caused by shear and $P_b$ the production–destruction caused by buoyancy. The constants in the turbulence model are denoted by $C_{1_\varepsilon}$, $C_{2_\varepsilon}$, $C_{3_\varepsilon}$ and $C_\mu$, respectively, and the values can be found in Table 3.

## DETAILS OF CALCULATIONS

All the relevant differential equations can formally be written as

$$\frac{\partial \phi}{\partial t} + \mathrm{div}(\overline{V}\phi) = \mathrm{div}(\Gamma\ \mathrm{grad}\ \phi) + S_\phi$$

where $\phi$ = dependent variable
$\overline{V}$ = water velocity
$\Gamma$ = exchange coefficient
$S_\phi$ = source and sink terms.

The four terms in this general equation are the unsteady term, the advective term, the diffusion term and the source–sink term. The dependent variable can stand for heat, salinity, frazil ice, frazil-flocs, momentum, turbulent kinetic energy or the dissipation rate of turbulent kinetic energy.

All conservation equations can thus be written in a similar way, which implies that our equations can be solved using the same numerical method. The boundary conditions may be specified in two different ways; either by prescribing the value or by prescribing the flux of the variable in question.

When discretizing the general differential equation, several schemes exist. The present author and his colleagues have used a control-volume formulation. The formulation starts by dividing the water body into control volumes around grid points and integrating the equation over these volumes. The discretized equation obtained in this manner thus concentrates on the conservation principle, and the discretization makes physical interpretations pos-

31

sible. For further discussions about the numerical scheme the reader is recommended to consult the book by Patankar (1980).

## RESULTS

In this section some of the results by the present author and his colleagues are given. In all calculations presented, two general equation solvers for hydrodynamic flows have been used, the PROBE program by Svensson (1979) for one-dimensional boundary layer problems and the PHOENICS program by Rosten et al. (1982) for the river applications.

### Laboratory simulations

There are today several important laboratory experiments on frazil ice formation available, e.g., those of Arakawa (1954), Carstens (1966), Mueller and Calkins (1978), Martin and Kauffman (1981), Ettema et al. (1984), Hanley and Tsang (1984), Tsang and Hanley (1985).

One main problem with these experiments is that the turbulent flows, under which the ice is formed, are often complex and difficult to simulate. The experiments are either conducted in a turbulence jar with a vertically oscillating grid or in flumes of racetrack shape, where the flow is driven by a propeller.

From a modeling point of view, we need experimental data from well-established boundary layer flows. The flume flow experiment probably meets this requirement in the best way; however, the turbulence generated by the propeller, side wall effects and secondary circulation complicate the flow.

In Omstedt (1985a), the laboratory experiments

of Tsang and Hanley (1985) were analyzed. In the numerical simulation, the frazil ice crystals were treated as thin, uniform plates. The heat transfer between the frazil ice and surrounding water was calculated from Fourier's law of heat conduction, with the heat transfer coefficient based upon a constant Nusselt number. The general experimental findings were well reproduced by the model. For example, the time for the temperature curve to reach 90% recovery from maximum supercooling, as well as the maximum supercooling, were numerically well simulated (Fig. 8).

The time evolution during initial frazil ice formation was studied by comparing model calculations with normalized data from Tsang and Hanley (1985). In Figure 9, the time evolutions of the normalized frazil ice concentrations during nine experiments are considered. The normalized parameters are the dimensionless time, defined as the ratio between time and characteristic time, and the dimensionless frazil ice concentration, defined as the ratio between frazil ice concentration and characteristic concentration. The characteristic time is defined as the time for the temperature curve to reach 90% recovery from maximum supercooling, and the characteristic concentration is defined as the frazil ice concentration at the characteristic time. The calculations reproduce the data quite well, except at the very first stage of the ice formation. This was attributed to the growth of the very first small crystals and was not dealt with by the model.

### Ocean simulations

In the ocean, frazil ice forms in at least four different situations (Martin 1981):
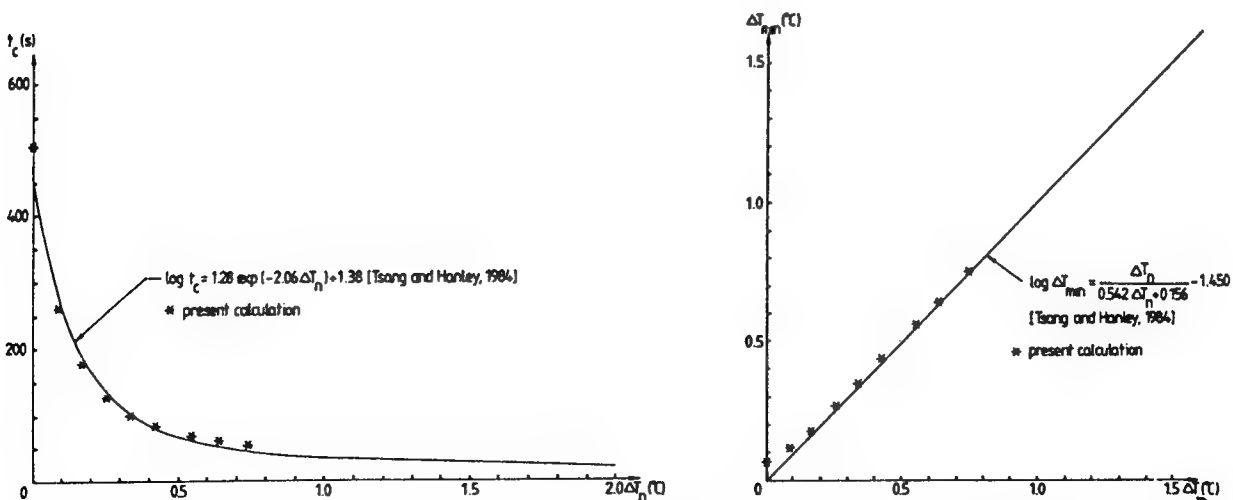


*Figure 8. Measured and calculated relationship between the characteristic time $t_c$, the temperature of maximum supercooling $\Delta T_{min}$ and the amount of supercooling at seeding $\Delta T_n$ (from Omstedt 1985a).*
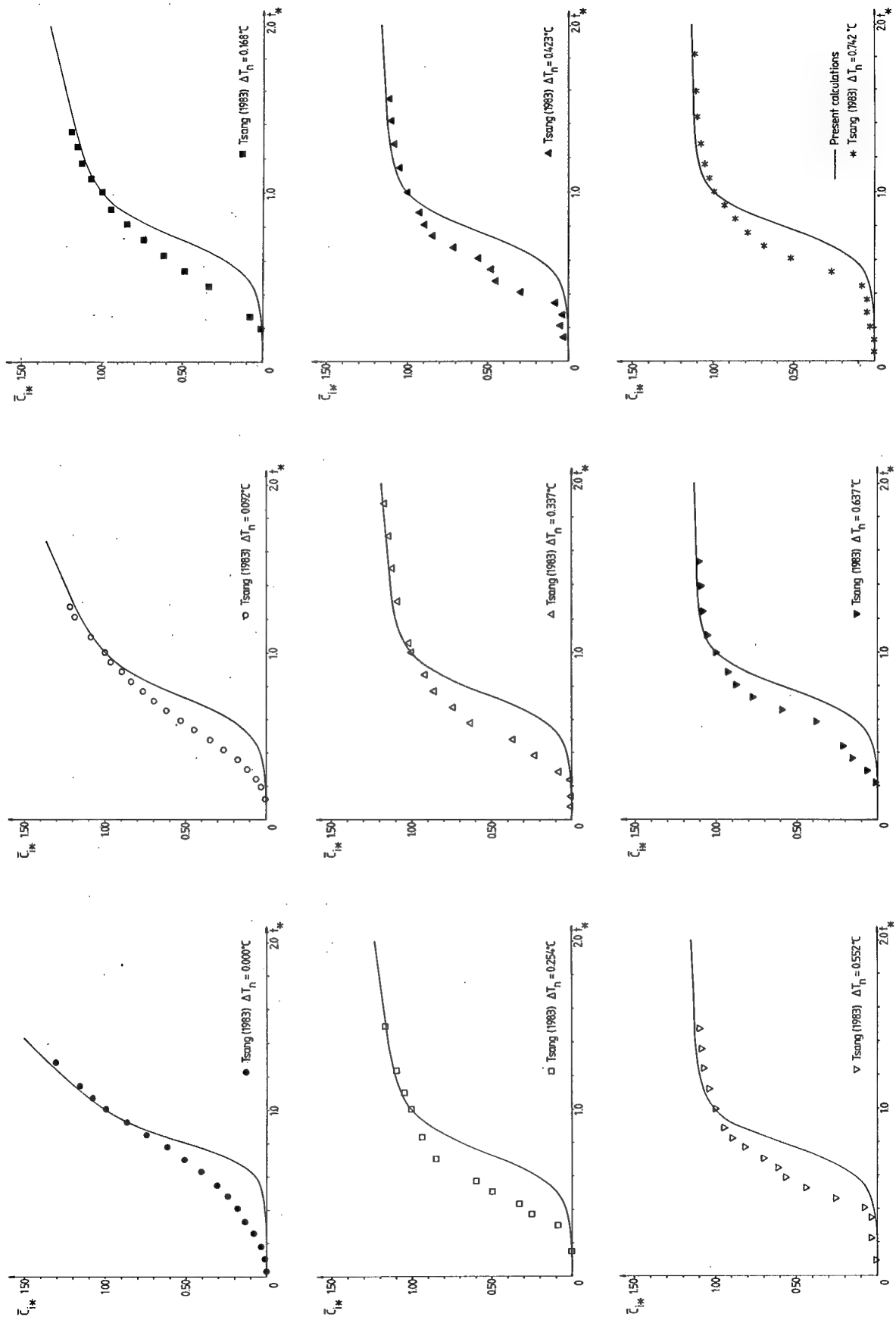
32

Figure 9. Measured and calculated relationship between the normalized frazil ice concentration $\bar{C}_{i*}$ and the normalized time $t_*$ (from Omstedt 1985a).

33

1. In open water areas, caused by a net heat loss to the atmosphere and similar to the process found in rivers.

2. At the interface between two fluid layers, each at its freezing point and with different salinities.

3. Below freezing sea ice, owing to the drainage of cold, dense brine associated with the ice growth.

4. Attached to ice shelves and icebergs and associated with rising sea water.

The importance of frazil ice for the sea ice cover in the Antarctic—the world's largest frazil ice producer—is further discussed by Lange (1990).

This chapter considers only frazil ice formation in open water areas. The general frazil ice equations, eq 30 and 31, with corresponding source-sink terms can, however, also be applied to the other situations. The pressure effects and the relevant mechanism of nucleation should then also be considered.

In the surface layers of the ocean, the mixed-layer dynamics play a very important role. With weak winds and stratified or shallow waters, ice can rapidly form over large areas. However, in deeper oceans ice may never form because of convection.

In Figure 10, the effect of wind mixing on supercooling and ice formation is illustrated. If the wind speed increases, warm water from deeper layers is mixed into the surface water, and the ice formation is delayed.

The effect of mass exchange on supercooling and ice formation is illustrated in Figure 11. It is interesting to note that, compared with high rates of mass exchange, low rates of mass exchange lead to higher supercooling and more rapid recovery times. This implies that even if the rate of mass exchange is modeled too low or too high, the dynamics tries to "correct" the time–temperature evolution.

In the model by Omstedt and Svensson (1984), the frazil ice crystals were treated as spheres with a mean radius of $10^{-3}$ m, and flocculation was not dealt with; instead, the calculation was terminated at a high frazil ice concentration. The model was extended in Omstedt (1985b), where the frazil ice crystals were treated as thin plates and flocculation of frazil ice crystals was considered.

Two basic differences between the calculations in Omstedt and Svens-
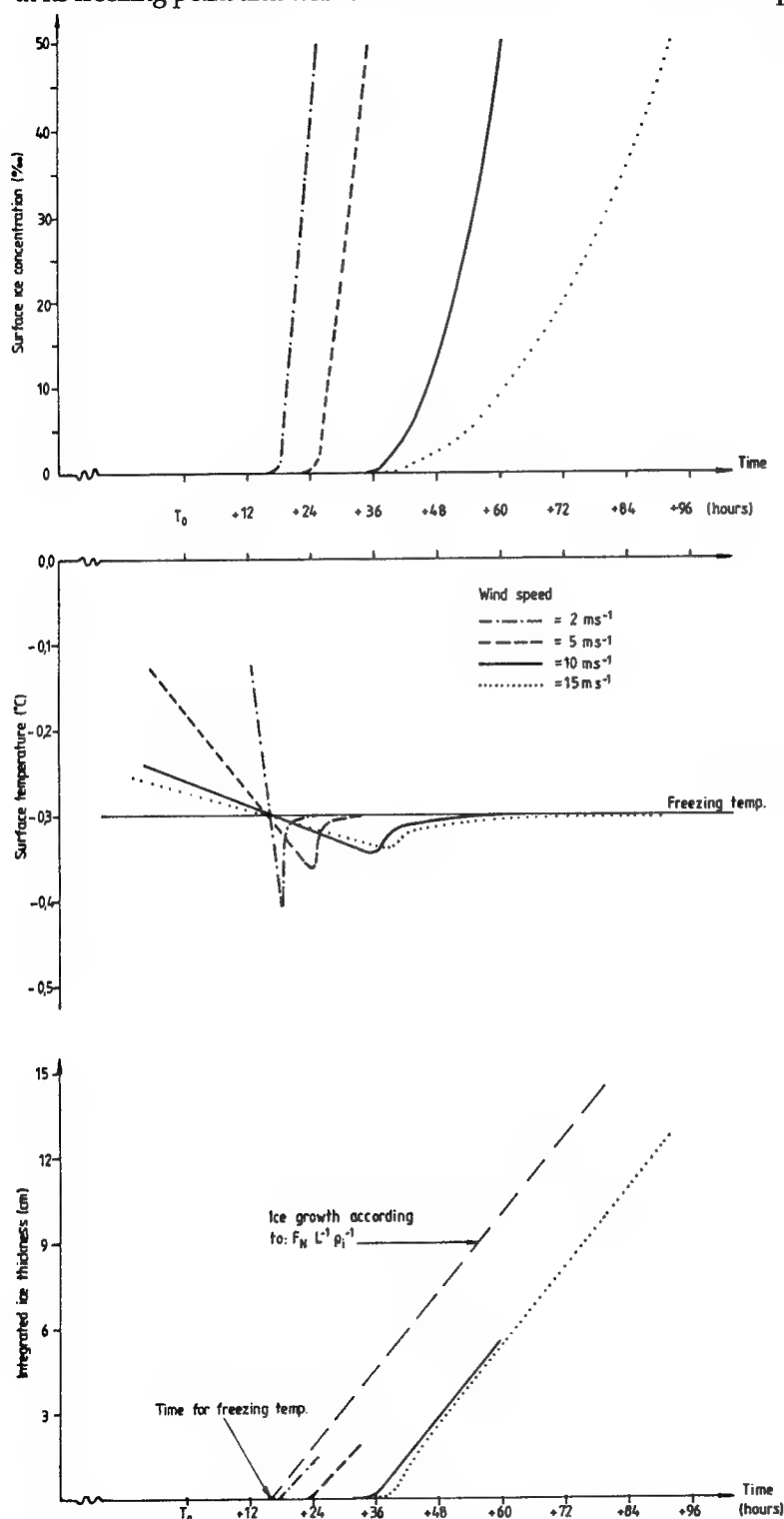


Figure 10. Effect of wind mixing on supercooling and initial ice formation (from Omstedt and Svensson 1984).

34

son (1984) and in Omstedt (1985b) were found. Firstly, the time–temperature response to frazil ice formation became more rapid (Fig. 12). Secondly, flocculation or grease ice formation started at lower frazil ice concentrations than was assumed in Omstedt and Svensson (1984). In fact, the calculations indicate that flocculation becomes important even for frazil ice concentrations below 1‰.

The amount of open water, and thus the area where surface frazil ice can form, is an intricate balance among ice drift, ice formation and melting. Polynyas, leads and the positions of ice fronts are the areas where this balance can be in favor of frazil ice formation. For a review of different aspects of sea ice the reader is referred to Untersteiner (1986).

### River simulations

In rivers the advection and the geometry play an important role. In some river reaches, the velocities are low, and shore ice can grow out and cover the reach. In other reaches, the water flow is faster, and frazil ice may form. Again, we have to understand the basic balances that form or break up the ice cover.

A frazil ice model for rivers was presented by Nyberg (1986). The simulation of frazil ice followed that by Omstedt (1985b), with some modifications. The modifications were that the flow was treated as a two-dimensional turbulent channel flow and that melting was considered as well as the formation of anchor ice. From some idealized calculations, Nyberg (1986) presented vertical, as well as downstream, distributions of temperature, frazil ice and frazil flocs (Fig. 13).

The model has been extended to a river reach in Sweden (Fig. 14). In this application, the river flow was treated as a transient three-dimensional channel flow, using body-fitted coordinates. The number of grid cells used was 1560, and the time step extended over a few minutes. A quasi-steady-state situation was reached after about 1 hour of simulation, which required about 20 minutes of CPU-time on a VAX 8600 computer. Applications of the model during two winter periods are further discussed by Sahlberg (1990).

The questions analyzed by the model simulations were: When and where will frazil ice form during different environmental conditions?
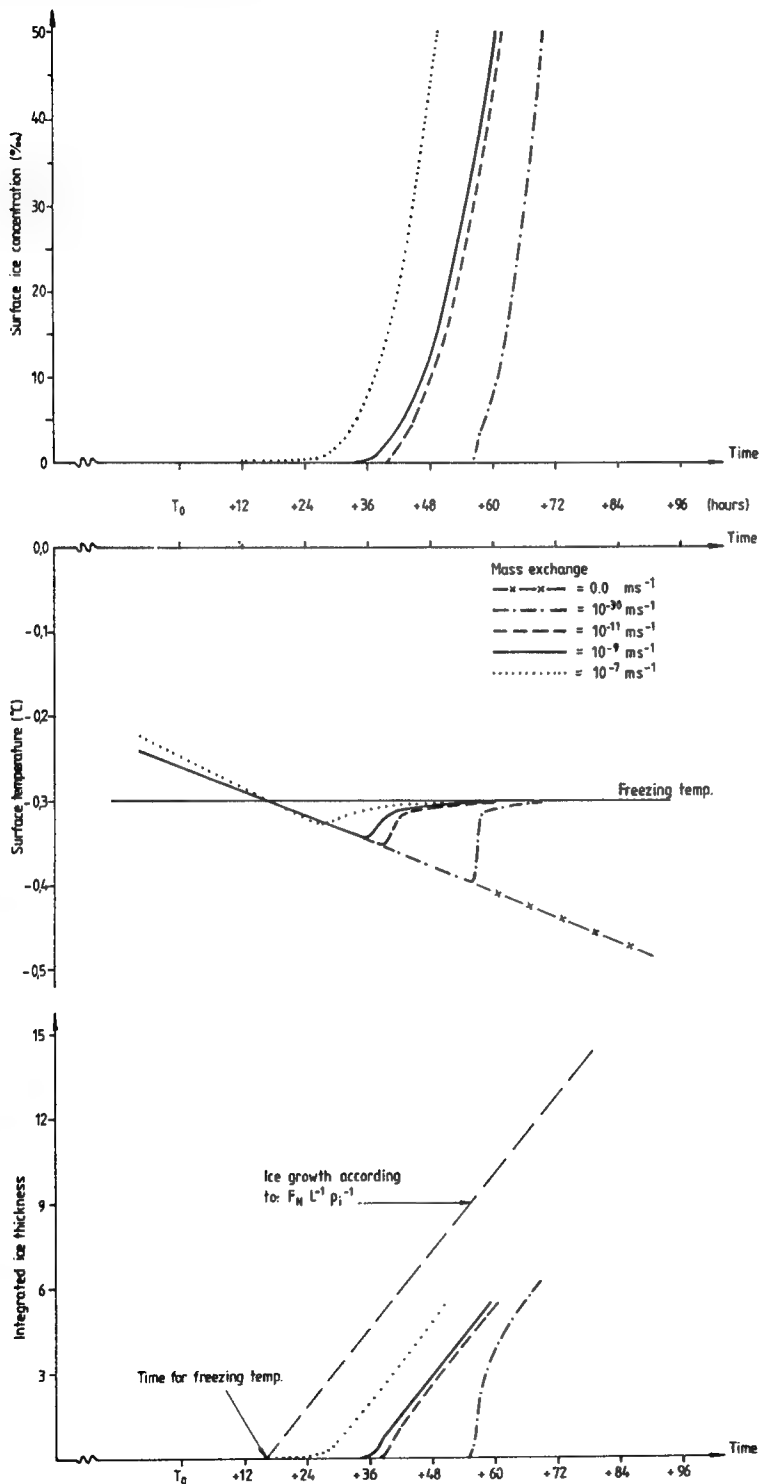


*Figure 11. Effect of mass exchange on supercooling and ice formation (from Omstedt and Svensson 1984).*
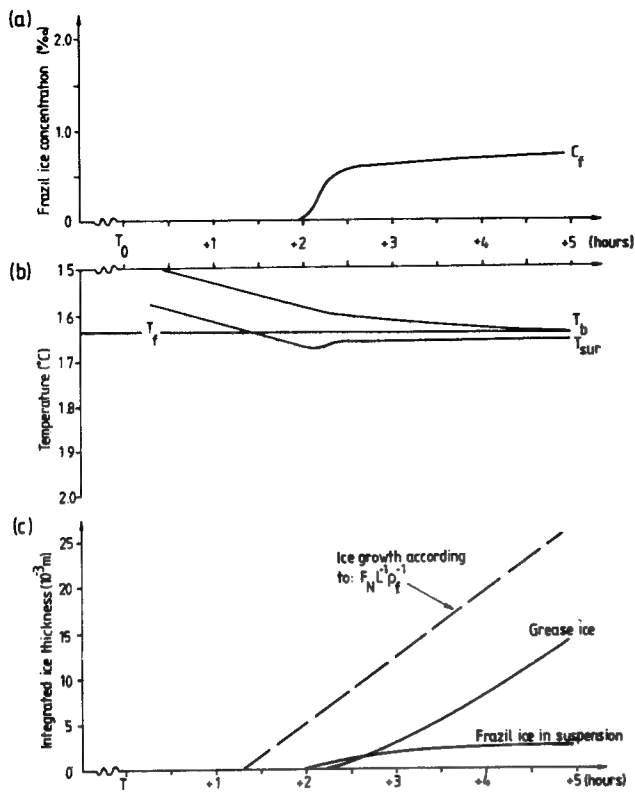
Figure 12. Water cooling and initial ice formation in an idealized ocean situation (from Omstedt 1985a).
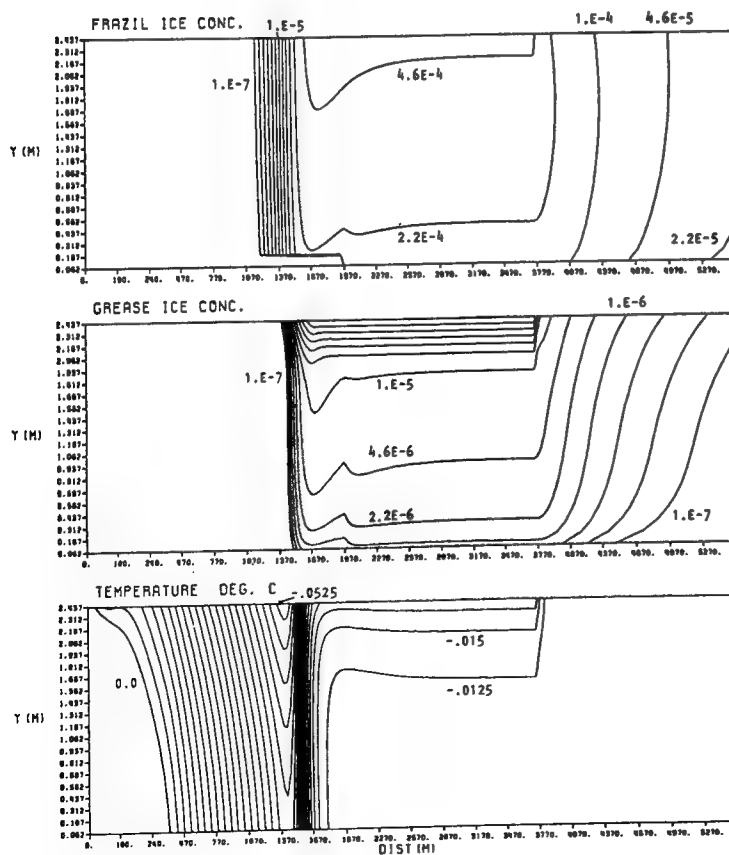


Figure 13. Water cooling and initial ice formation in an idealized river situation (from Nyberg 1986).
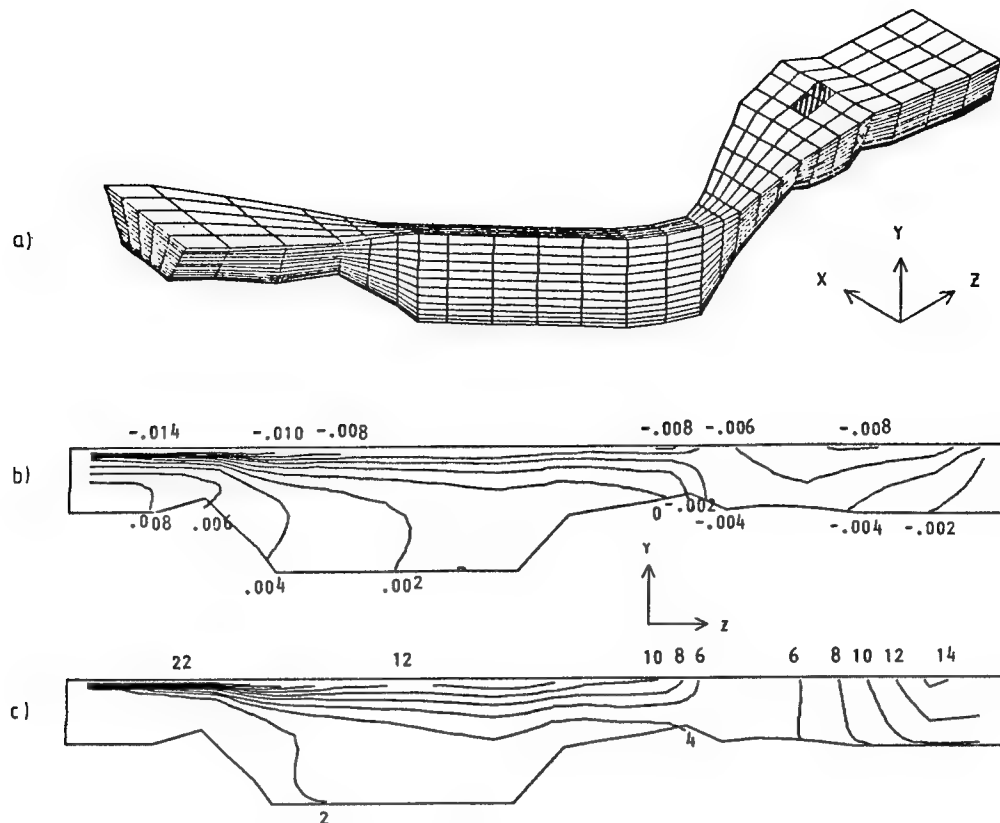
*Figure 14. Frazil ice formation in Stornorrfors—an example. The discharge is 600 m³/s, the inflow temperature is 0.01 °C and the net heat loss is 450 W/m² (from Nyberg 1987). a—Grid net, b—Calculated water temperature ( °C), c— Calculated frazil ice concentration ($C_f/10^{-5}$).*

## FORECASTS

In this section, the problem of forecasting frazil ice is discussed. Any forecasting of the onset of frazil ice will rely on successfully predicting the cooling rate. In oceans and rivers, models for predicting water cooling are available (see, e.g., Omstedt 1984, 1990, Shen et al. 1984). The results from these applications are encouraging.

In this discussion it is important to distinguish between diagnostic studies and forecast studies. In general, the main studies in the literature about cooling are diagnostic, meaning that the time–temperature evolutions are simulated on the basis of measured weather data. The forecast studies include a further complication associated with the uncertainty in the weather parameters.

For the prediction of the onset of frazil ice formation, some diagrams are available (Ginsburg 1979). The diagrams are probably quite site-specific and should therefore be further developed. One way of doing this is to use an advanced frazil ice model and develop local diagrams for the wa-

ter body of interest. Basic parameters in these diagrams should be:
1. Upstream temperature
2. Discharge–volume flow
3. Air temperature
4. Wind
5. Cloudiness
6. Humidity
7. Amount of open water.

The list above indicates that somewhat complicated diagrams have to be constructed, but for specific locations they may probably serve as useful tools.

The main elements in a forecasting system are the following:
1. A budget for the heat exchange between the air/water and the water/bottom interfaces.
2. A hydrodynamic model, including the temperature equation.
3. A frazil ice model, including the mass exchange with the atmosphere.
4. An ice cover model, predicting the amount of open water.

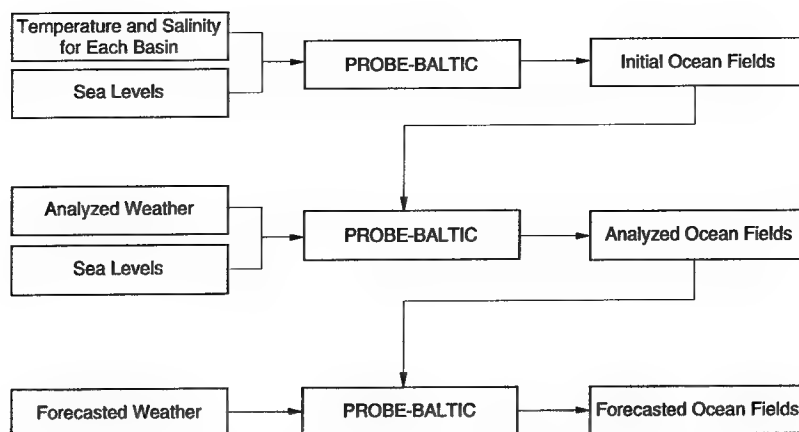The forecaster needs the following initial data:

Temperature and Salinity for Each Basin

Sea Levels

PROBE-BALTIC → Initial Ocean Fields

Analyzed Weather

Sea Levels

PROBE-BALTIC → Analyzed Ocean Fields

Forecasted Weather → PROBE-BALTIC → Forecasted Ocean Fields

*Figure 15. How oceanographic and meteorological data can be combined with mathematical models (after Omstedt 1990).*

1. Initial temperatures and salinities.
2. Initial upstream temperatures and discharge–volume flow.
3. Initial distribution of open water areas.

The strategy when forecasting the frazil ice formation will depend upon the specific water body studied. However, the forecaster needs to be well integrated with the weather forecasting service. Owing to the limited number of temperature and ice cover data, etc., available, which are necessary for starting up any calculations, the forecasts often need to be supplemented with updating calculations. These calculations, based on observed weather, wind and ice conditions, should then produce the necessary starting values for the forecasts (Omstedt 1990).

In Figure 15, the model structure of a forecasting system for water temperatures applied to the Baltic Sea is illustrated. The model (PROBE-BALTIC) is used in two modes. The first one, the real-time mode, fits the oceanographical and meteorological data collected in the recent past to the model. The second one, the forecast mode, starts from the real-time mode, and calculates the forecasts.

## DISCUSSION

The purpose of this chapter was to review the numerical modeling of frazil ice in water bodies. Few models are available, but it is believed that the model approach given by the present author and his colleagues forms a good base for further research and also for applications to different water bodies. More efforts need to be applied to modeling and measuring frazil ice and particularly to the crystal number continuity equation (see further discussion in Svensson and Omstedt [1994]).

In diagnostic studies, all equations should be used, and diagrams for specific areas could be constructed. When developing forecast systems, the choice between diagrams and numerical models will be a question of how accurate the forecast requirements are. The accuracy of any frazil ice forecast is probably as accurate as the water cooling forecast allows it to be. This may therefore guide the choice of model complexity when developing forecast systems for frazil ice.

# LITERATURE CITED

**Abramenkov, N.M.** (1980) Use of the kinetic equation for describing the formation of frazil. *Meteorology and Hydrology,* **9**: 77–83.

**Andreas, E.L and B. Murphy** (1986) Bulk transfer coefficients for heat and momentum over leads and polynyas. *Journal of Physical Oceanography,* **16**: 1875–1883.

**Arakawa, K.** (1954) Studies on the freezing of water. II. Formation of disc crystals. *Journal of the Faculty of Science, Hokkaido University,* Series **II, IV**(5):310–339.

**Arden, R.S. and T.E. Wigle** (1972) Dynamics of ice formation in the Upper Niagara River. In *Proceedings, International Symposium on the Role of Snow and Ice in Hydrology, Banff, Alberta,* vol. 2. UNESCO-WMO-IHAS.

**Ashton, G.D., Ed.** (1986) *River and Lake Ice Engineering.* Littleton, Colorado: Water Resources Publications.

**Bauer, J. and S. Martin** (1983) A model of grease ice growth in small leads. *Journal of Geophysical Research,* **88**: 2917–2925.

**Beltaos, S. and A.M. Dean, Jr.** (1981) Field investigation of a hanging ice dam. In *Proceedings, International Association for Hydraulic Research Symposium on Ice, 27–31 July, Quebec City,* vol 2, p. 475–488.

**Botsaris, G.D.** (1976) Secondary nucleation—A review. In *Industrial Crystallization* (J.W. Mullin, Ed.). New York: Plenum Press.

**Bukina, L.A.** (1963) On the relation between temperature and ratio of thickness diameter of frazil ice crystals of disk-like form. *Bull. Acad. Sci., Geophys, Ser.*

**Caldwell, D.R.** (1978) The maximum density points of pure and saline water. *Deep-Sea Research,* **25**: 175–181.

**Carstens, T.** (1966) Experiments with supercooling and ice formation in flowing water. *Geofysiske Publikasjoner,* **26**(9): 1–17.

**Carstens, T.** (1970) Heat exchanges and frazil formation. In *Proceedings, International Association for Hydraulic Research Symposium on Ice, Reykjavik, Iceland.*

**Chacho, E., D. Lawson and B. Brockett** (1986) Frazil ice pebbles: Frazil ice aggregates in the Tanana River near Fairbanks, Alaska. In *Proceedings, International Association for Hydraulic Research Symposium on Ice, 18–22 August, Iowa City.*

**Cise, M.D. and A. Randolph** (1972) Secondary nucleation of potassium sulphate in a continuous flow, seeded crystallizer. *American Institute of Chemical Engineers Symposium Series,* **68**(121).

**Cooper, W.A.** (1974) A possible mechanism for contact nucleation. *Journal of Atmospheric Science,* **31**.

**Daly, S.F.** (1984) Frazil ice dynamics. USA Cold Regions Research and Engineering Laboratory, Monograph 84-1.

**Daly, S.F. and K.D. Axelson** (1989) Estimation of time to maximum supercooling during dynamic frazil ice formation. USA Cold Regions Research and Engineering Laboratory, Special Report 89-26.

**Daly, S.F. and K.D. Axelson** (1990) Stability of floating and submerged blocks. *Journal of Hydraulic Research,* **28**(6): 737–752.

**Daly, S.F. and S. Colbeck** (1986) Frazil ice measurements in CRREL's flume facility. In *Proceedings, International Association for Hydraulic Research Symposium on Ice, 18–22 August, Iowa City,* vol. 1, p. 427–438.

**Danard, M., M. Gray and G. Lyv** (1983) A model for the prediction of initial sea ice formation. *Monthly Weather Review,* **111**(8): 1634–1546.

**Dufour, L. and R. Defay** (1963) *Thermodynamics of Clouds.* New York: Academic Press.

**Ettema, R., M.F. Karim and J.F. Kennedy** (1984) Frazil ice formation. USA Cold Regions Research and Engineering Laboratory, CRREL Report 84-18.

**Evans, T.W., G. Margolis and A.F. Sarofim** (1974a) Mechanisms of secondary nucleation in agitated crystallizers. *American Institute of Chemical Engineers Journal,* **20**(5): 950–958.

**Evans, T.W., A.F. Sarofim and G. Margolis** (1974b) Models of secondary nucleation attributable to crystal–crystallizer and crystal–crystal collisions. *American Institute of Chemical Engineers Journal,* **20**(5): 950–958.

**Fletcher, N.H.** (1968) Ice nucleating behaviour of silver iodide smokes containing a soluble component. *Journal of Atmospheric Sciences,* **25**.

**Forest, T.W.** (1986) Thermodynamic stability of frazil ice crystals. In *Proceedings, American Society of Mechanical Engineers Fifth International Symposium on Offshore Mechanics and Arctic Engineering, Tokyo.*

**Freysteinsson, S.** (1970) Calculation of frazil ice production. In *Proceedings, International Association for Hydraulic Research Symposium on Ice, Reykjavik, Iceland.*

**Fujioka, T.** (1978) Study of ice growth in slightly undercooled water. Ph.D. Dissertation, Carnegie-Mellon University (unpublished).

**Fujioka, T. and R.F. Sekerka** (1974) Morphological stability of disc crystals. *Journal of Crystal Growth,* **24**.

**Garabedian, H. and R.F. Strickland-Constable** (1974) Collision breeding of ice crystals. *Journal of Crystal Growth,* **22**: 188–192.

**Garside, J. and M.A. Larson** (1978) Direct observa-

tion of secondary nuclei production. *Journal of Crystal Growth*, **43**.

Gill, A.E. (1982) *Atmosphere-Ocean Dynamics. International Geophysical Series*, vol. 30. New York: Academic Press.

Ginsburg, B.M. (1979) Methods of short-term forecasts of frazil ice. WMO Technical Report to the Commission for Hydrology, p. 1–9.

Gosink, J.P. and T.E. Osterkamp (1983) Measurements and analyses of velocity profiles and frazil ice-crystal rise velocities during periods of frazil-ice formation in rivers. *Annals of Glaciology* **4**: 79–84.

Gosink, J.P. and T. Osterkamp (1986) Frazil ice nucleation by ejecta from supercooled water. In *Proceedings, International Association for Hydraulic Research Symposium on Ice, 18–22 August, Iowa City.*

Gunaratna, P. (1989) Simulation of hydraulics and thermal-ice regimes in river networks. Ph.D. Dissertation. Potsdam, New York: Department of Civil and Environmental Engineering, Clarkson University (unpublished).

Hanley, T.O'D. and B. Michel (1977) Laboratory formation of border ice and frazil slush. *Canadian Journal of Civil Engineering*, **4**: 153–160.

Hanley, T.O'D., and G. Tsang (1984) Formation and properties of frazil ice in saline water. *Cold Regions Science and Technology*, **8**(3): 209–221.

Hillig, W.B. (1958) The kinetics of freezing. In *Growth and Perfection of Ice Crystals* (R.H. Doremus, B.W. Roberts and D. Turnbull, Ed.). New York: John Wiley and Son.

Ho, C.F. (1990) A two-dimensional free drift model for river ice cover formation. Ph.D. Dissertation. Potsdam, New York: Department of Civil and Environmental Engineering, Clarkson University (unpublished).

Hopkins, M. and X. Lange (1991) Inelastic microstructure in rapid granular flows of smooth discs. *Physics of Fluids A*, **3**(1): 47–57.

Hopper, H.R., et al. (1980) Hanging dams in the Manitoba Hydro System. In *Proceedings, Workshop on Hydraulic Resistance of River Ice, 23–24 September, Burlington, Ontario* (G. Tsang and S. Beltaos, Ed.). Burlington, Ontario: National Water Research Institute, p. 195–208.

Jackson, K.A. (1958) A possible mechanism for contact nucleation. *Journal of Atmospheric Sciences*, **31**.

Jackson, K.A., D.R. Uhlmann and J.D. Hunt (1967) On the nature of crystal growth from the melt. *Journal of Crystal Growth*, **1**: 1–36.

Kempema, E.W., E. Reimnitz and R.E. Hunter (1986) Flume studies and field observations of the interaction of frazil ice and anchor ice with sediments. U.S. Geological Service, Open-File Report 86-515.

Kempema, E.W., E. Reimnitz, J.R. Clayton, Jr. and J.R. Payne (1993) Interactions of frazil and anchor ice with sedimentary particles in a flume. *Cold Regions Science and Technology*, **21**: 137–149.

Kristinsson, B. (1970) Ice monitoring equipment. In *Proceedings, International Association for Hydraulic Research Symposium on Ice, Reykjavik, Iceland*, Paper 1.1.

Kumai, M. and K. Itagaki (1953) Cinematographic study of ice crystal formation in water. *Journal of the Faculty of Science, Hokkaido University*, Series II, **IV**(4): 234–246.

Lal, A.M.W. (1989) A mathematical model for river ice processes. Ph.D. Dissertation. Potsdam, New York: Department of Civil Environment Engineering, Clarkson University (unpublished).

Lange, M.A. (1990) Properties of sea ice in the Weddell Sea, Antarctica. In *Proceedings, International Association for Hydraulic Research Symposium on Ice, 20–23 August, Espoo, Finland*, vol. 1, p. 289–299.

Lever, J.H., S.F. Daly, J.H. Rand and D. Furey (1992) A frazil concentration meter. In *Proceedings, International Association of Hydraulic Research Symposium on Ice, 15–19 June, Banff, Alberta*, p. 1362–1376.

Lindow, S.E., C.D. Arny, C.D. Upper and W.R. Barchett (1978) The role of bacteria ice nuclei in frost injury to sensitive plants. In *Plant Cold Hardiness and Freezing Stress-Mechanisms and Crop Implications* (P.H. Li and A. Sakai, Ed.). New York: Academic Press, p. 249–263.

Liou, C.P. and M.G. Ferrick (1992) A model for vertical frazil distribution. USA Cold Regions Research and Engineering Laboratory, CRREL Report 92-4.

Marcotte, N., and S. Robert (1986) Elementary mathematical modelling of anchor ice. In *Proceedings, International Association for Hydraulic Research Symposium on Ice, Iowa City*, vol. 1, p. 493–506.

Margolis, G. (1969) The nucleation and growth rates of ice in a well-stirred crystallizer. Ph.D. Dissertation. Cambridge, Massachusetts: Department of Chemical Engineering, Massachusetts Institute of Technology (unpublished).

Martin, S. (1981) Frazil ice in rivers and oceans. *Annual Review of Fluid Mechanics*, **13**: 379–397.

Martin, S., and P. Kauffman (1981) A field and laboratory study of wave damping by grease ice. *Journal of Glaciology*, **27**: 281–314.

Matousek, V. (1981) A mathematical model of the discharge of frazil in rivers. In *Proceedings, International Association for Hydraulic Research Symposium on Ice, 27–31 July, Quebec City.*

Matousek, V. (1984) Types of ice run and conditions for their formation. In *Proceedings, International Association for Hydraulic Research Symposium on Ice, Hamburg, Germany, 27–31 August*, p. 315–327.

McGilvary, W.R. and B. Coutermarsh (1992) Dynamic analysis of ice floe underturning stability. In *Proceedings, International Association for Hydraulic Research Symposium on Ice, 15–19 June, Banff, Alberta.*

Mellor, G.L., M.G. McPhee and M. Steele (1986) Ice–sea water turbulent boundary layer interaction with melting or freezing. *Journal of Physical Oceanography,* 16: 1829–1846.

Mercier, R. (1984) The reactive transport of suspended particles: Mechanisms and modeling. Ph. D. Dissertation. Cambridge: Joint Committee on Oceanographic Engineering, Massachusetts Institute of Technology (unpublished).

Michaels, A.S., P.L.T. Brian and P.R. Sperry (1966) Impurity effects on the basal plane solidification kinetics of supercooled water. *Journal of Applied Physics.*

Michel, B. (1963) Theory of formation and deposit of frazil ice. In *Proceedings, Annual Eastern Snow Conference, Quebec City, Quebec,* p. 130–148.

Michel, B. (1971) Winter regime of rivers and lakes. USA Cold Regions Research and Engineering Laboratory, Monograph III-B1a.

Michel, B. (1978) *Ice Mechanics.* Quebec: Les Presses de L'University Laval.

Michel, B. (1984) Comparison of field data with theories on ice cover progression in large rivers. *Canadian Journal of Civil Engineering,* 11: 798–814.

Michel, B. (1986) Packing in front of a forming ice cover. In *Proceedings, International Association for Hydraulic Research Symposium on Ice, 18–22 August, Iowa City,* p. 75–88.

Michel, B. (1990) Impact of dams on the ice regime of rivers. In *Proceedings, International Association for Hydraulic Research Symposium on Ice, 20–23 August, Espoo, Finland,* vol. 2, p. 690–696.

Michel, B. (1991) Critical physical processes in the numerical modeling of river ice. In *Proceedings of the 6th Workshop on the Hydraulics of River Ice, 23–25 October, Ottawa, Ontario,* p. 91–112.

Michel, B. and M. Drouin (1975) Equilibrium of an underhanging dam at the La Grande River. Quebec: Department de Genie Civil, Universitè Laval.

Michel, B., et al. (1981) Backwater curves under ice cover of the La Grande River (in French with English summary). *Canadian Journal of Civil Engineering,* 8(3): 351–363.

Mossop, S.C. (1955) The freezing of supercooled water. *Proceedings of the Physical Society,* 68: 193.

Mueller, A. (1978) Frazil ice formation in turbulent flow. The University of Iowa, Iowa Institute of Hydraulic Research, Report No. 214.

Mueller, A., and D.J. Calkins (1978) Frazil ice formation in turbulent flow. In *Proceedings, International Association for Hydraulic Research Symposium on Ice, 7–9 August, Lulea, Sweden.*

Nyberg, L. (1986) Ice formation in rivers. In *Numerical Simulation of Fluid Flow and Heat/Mass Transfer Processes* (C.A. Brebbia and S.A. Orszag, Ed.). Lecture notes in engineering, No. 18. Springer-Verlag, p. 108–121.

Nyberg, L. (1987) Modelling frazil ice formation in a channel flow (in Swedish). HOF PM No. 56. Norrköping, Sweden: SMHI.

Omstedt, A. (1984) A forecast model for water cooling in the Gulf of Bothnia and Lake Vänern. SMHI Report No. RHO 36. Norrköping, Sweden: SMHI.

Omstedt, A. (1985a) On supercooling and ice formation in turbulent sea water. *Journal of Glaciology,* 31(109): 263–271.

Omstedt, A. (1985b) Modelling frazil ice and grease ice in the upper layers of the ocean. *Cold Regions Science and Technology,* 11: 87–98.

Omstedt, A. (1986) Modelling initial ice formation in rivers and oceans. In *Proceedings, International Association for Hydraulic Research Symposium on Ice, Iowa City,* vol. 1, p. 559–568.

Omstedt, A. (1990) Real time modeling and forecasting of temperature in the Baltic Sea. SMHI Report No. 12. Norrköping, Sweden: SMHI.

Omstedt, A., and U. Svensson (1984) Modelling supercooling and ice formation in a turbulent Ekman layer. *Journal of Geophysical Research,* 89(C1): 735–744.

Osterkamp, T.E. (1977) Frazil-ice nucleation by mass-exchange processes at the air/water interface. *Journal of Glaciology,* 19(81): 619–625.

Osterkamp, T.E. (1978) Frazil ice formation: A review. *ASCE, Journal of the Hydraulics Division,* 104(HY9): 1239–1253.

Osterkamp, T.E. and J.P. Gosink (1982) A photographic study of frazil and anchor ice formation, frazil ice evolution and ice cover development in interior Alaska stream. Fairbanks: Geophysical Institute, University of Alaska.

Osterkamp, T.E., C.S. Benson, R.E. Gilfilian and T. Ohtake (1973) Winter history of an Alaska stream. In Annual Report of the Geophysical Institute, University of Alaska, Fairbanks.

Osterkamp, T.E., T. Ohtake and D.C. Warniment (1974) Detection of airborne ice crystals near a supercooled stream. *Journal of Atmospheric Sciences,* 31.

Pariset, E. and R. Hausser (1961) Formation and evolution of ice covers on rivers. *Transactions, Engineering Institute of Canada,* 5(1): 41–49.

Patankar, S.V. (1980) *Numerical Heat Transfer and Fluid Flow.* New York: McGraw-Hill Book Company.

Pease, C. (1987) The surge of wind-driven coastal polynyas. *Journal of Geophysical Research,* 92: 7049–7059.

41

Pruppacher, H.R. and J.D. Klett (1978) *Microphysics of Clouds and Precipitation.* Dordrecht: D. Reidel.

Rodi, W. (1980) Turbulence models and their application in hydraulics—A state of the art review. Report from the IAHR Section of Fundamentals of Division II: Experimental and Mathematical Fluid Dynamics.

Rodi, W. (1987) Examples of calculation methods for flow mixing in stratified flows. *Journal of Geophysical Research*, **92**: 5305–5328.

Rosten, H.I., D.B. Spalding and D.G. Tatchell (1982) PHOENICS—An instruction manual. London: CHAM Limited.

Sahlberg, J. (1990) Frazil ice problems at Stornornfors water power plant in the Une River. In *Proceedings, International Association for Hydraulic Research Symposium on Ice, 20–23 August, Espoo, Finland,* vol. 1, p. 427–441.

Schaefer, V.J. (1950) The formation of frazil and anchor ice in cold water. *Transactions of the American Geophysical Union,* **31**.

Shen, H.T., E.P. Foltyn and S.F. Daly (1984) Forecasting water temperature decline and freeze-up in rivers. USA Cold Regions Research and Engineering Laboratory, CRREL Report 84-19.

Shen, H.T., et al. (1984) Field investigation of St. Lawrence River hanging ice dams. In *Proceedings, International Association for Hydraulic Research Symposium on Ice, 27–31 August, Hamburg, Germany,* vol. 1, p. 241–249.

Smith, K.A. and A.F. Sarofim (1979) Fundamental studies of desalination by freezing. Final Report to Office of Water Research and Technology, U.S. Department of Interior, Washington, D.C.

Starosolszky, O. (1981) Thermal regime and ice forecasting for fresh-water bodies. In *Proceedings, International Association for Hydraulic Research Symposium on Ice, Quebec City.*

Steele, M., G.L. Mellor and M.G. McPhee (1989) Role of the molecular sublayer in the melting or freezing of sea ice. *Journal of Physical Oceanography,* **19**(1): 139–147.

Strickland-Constable, R.F. (1972) The breeding of crystal nuclei—A review of the subject. *American Institute of Chemical Engineers Symposium Series,* **68** (121).

Sun, Zhao-Chu and H.T. Shen (1988) A field investigation of frazil ice jam in Yellow River. In *Proceedings of the 5th Workshop on Hydraulics of River Ice/Ice Jams, June, Winnipeg, Manitoba,* p. 157–175.

Svensson, U. (1979) The structure of the turbulent Ekman layer. *Tellus,* **31**: 340–350.

Svensson, U. and A. Omstedt (1994) Simulation of supercooling and size distribution in frazil ice dynamics. *Cold Regions Science and Technology,* **22**: 221–233.

Tesaker, E. (1975) Accumulation of frazil ice in an intake reservoir. In *Proceedings, International Association for Hydraulic Research Symposium on Ice, 18–21 August, Hanover, New Hampshire,* p. 25–38.

Tsang, G. (1986) Preliminary report on field study at Cachine Rapids on cooling of river and formation of frazil and anchor ice. In *Proceedings, Fourth Workshop on Hydraulics of River Ice, June, Montreal, Canada,* vol. II.

Tsang, G. (1988) A theory for frazil distribution in turbulent flow. In *Proceedings, International Association for Hydraulic Research Symposium on Ice, 23–27 August, Sapporo, Japan.*

Tsang, G., and T.O'D. Hanley (1985) Frazil formation in water of different salinities and supercoolings. *Journal of Glaciology,* **31**(108): 74–85.

Turnbull, D. and J.C. Fisher (1949) Rate of nucleation in condensed systems. *Journal of Chemical Physics,* **17**: 71.

Untersteiner, N., Ed. (1986) The geophysics of sea ice. *The NATO ASI Series,* vol. B146. New York: Plenum Publishing Corp.

Wadia, P.H. (1974) Mass transfer from spheres and discs in turbulent agitated vessels. Ph.D. Dissertation. Cambridge: Department of Chemical Engineering, Massachusetts Institute of Technology (unpublished).

Weeks, W.F., and S.F. Ackley (1982) The growth, structure and properties of sea ice. USA Cold Regions Research and Engineering Laboratory, Monograph 82-1.

White, K.D. (In prep.) Frazil flow strength measurements: Preliminary tests. In *Proceedings of the Seventh Workshop on Hydraulics of ice Covered Rivers: Environmental Aspects of River Ice, 18-20 August, Saskatoon, Saskatchewan, Canada.*

Williamson, R.B. and B. Chalmers (1966) Morphology of ice solidified in undercooled water. In *Crystal Growth* (H.S. Peiser, Ed.). New York: Pergamon Press.

Wuebben, J.L. (1984) The rise pattern and velocity of frazil ice. In *Proceedings, Workshop on Hydraulics of River Ice, Fredricton, NB, Canada,* p. 297–314.

Yen, Y.-C. (1981) Review of thermal properties of snow, ice and sea ice. USA Cold Regions Research and Engineering Laboratory, CRREL Report 81-10.

# SELECTED BIBLIOGRAPHY

**Altberg, W.J.** (1936) Twenty years of work in the domain of underwater ice formation (1915–1935). International Union of Geodesy and Geophysics, International Association for Scientific Hydrology, Bulletin no. 23, p. 373–407.

**ASCE Task Committee on Hydromechanics of Ice of the Committee on Hydromechanics** (1974) River ice problems: A state-of-the-art survey and assessment of research needs. *Journal of the Hydraulics Division, ASCE,* **HY1**: 1–15.

**Barnes, H.T.** (1928) *Ice Engineering.* Montreal: Renouf Publishing Co.

**Coutermarsh, B. and R. McGilvary** (in prep.) Floating ice flow stability analysis. USA Cold Regions Research and Engineering Laboratory, CRREL Report.

**Devik, O.** (1930) Thermische und dynamische Bedingungen der Eidbildung in Wasserlaufen (in German). *Geofysiske Publikasjoner,* **IX**( 1).

**Devik, O.** (1942) Supercooling and ice formation in open waters. *Geofysiske Publikasjoner,* **XIII**(8).

**Devik, O.** (1944) Ice formation in lakes and rivers. *The Geographical Journal,* **5**.

**Devik, O. and E. Kanavin** (1963) *Oversikt over isproblemer i norske vassdrag.* Oslo (in Norwegian).

**Kristensen, I.** (1904) Isdannelsen i vore vassdrag. *3die norske landsmøde for teknik, Trondheim.*

**Murphy, J.** (1909) The ice question—as it affects Canadian water power—with special reference to frazil and anchor ice. *Transactions of the Royal Society of Canada,* **Section III**: 143–177.

**Osterkamp, T.E., R.E. Gilfilian and C.S. Benson** (1975) Observations of stage, discharge, pH, and electrical conductivity during periods of ice formation in a small subarctic stream. *Water Resources Research,* **112**: 268–272.

**Osterkamp, T.E., R.E. Gilfilian, J.P. Gosink and C.S. Benson** (1983) Water temperature measurements in turbulent streams during periods of frazil ice formation. *Annals of Glaciology,* **4**: 209–215.

**Shen, H.T.** (1980) Surface heat loss and frazil production in the St. Lawrence River. *Water Resources Bulletin,* **16**(6): 996–1001.

**Shen, H.T. and R.W. Ruggles** (1982) Winter heat budget and frazil ice production in the Upper St. Lawrence River. *Water Resources Bulletin,* **18**(2): 251–257.

**Williams, G.P.** (1959) Frazil ice: A review of its properties, with a selected bibliography. *The Engineering Journal,* **42**(11): 55–60.

# REPORT DOCUMENTATION PAGE

Public reporting burden for this collection of information is estimated to average 1 hour per response, including the time for reviewing instructions, searching existing data sources, gathering and maintaining the data needed, and completing and reviewing the collection of information. Send comments regarding this burden estimate or any other aspect of this collection of information, including suggestion for reducing this burden, to Washington Headquarters Services, Directorate for Information Operations and Reports, 1215 Jefferson Davis Highway, Suite 1204, Arlington, VA 22202-4302, and to the Office of Management and Budget, Paperwork Reduction Project (0704-0188), Washington, DC 20503.

| 1. AGENCY USE ONLY (Leave blank) | 2. REPORT DATE<br>August 1994 | 3. REPORT TYPE AND DATES COVERED |
|---|---|---|

**4. TITLE AND SUBTITLE**

International Association for Hydraulic Research
Working Group on Thermal Regimes:
Report on Frazil Ice

**5. FUNDING NUMBERS**

**6. AUTHORS**

Steven F. Daly, Editor

**7. PERFORMING ORGANIZATION NAME(S) AND ADDRESS(ES)**

International Association for Hydraulic Research
Working Group on Frazil Ice

**8. PERFORMING ORGANIZATION REPORT NUMBER**

Special Report 94-23

**9. SPONSORING/MONITORING AGENCY NAME(S) AND ADDRESS(ES)**

U.S. Army Cold Regions Research and Engineering Laboratory
72 Lyme Road
Hanover, New Hampshire 03755-1290

**10. SPONSORING/MONITORING AGENCY REPORT NUMBER**

**11. SUPPLEMENTARY NOTES**

**12a. DISTRIBUTION/AVAILABILITY STATEMENT**

Approved for public release; distribution is unlimited.

Available from NTIS, Springfield, Virginia 22161

**12b. DISTRIBUTION CODE**

**13. ABSTRACT (Maximum 200 words)**

This report, prepared by members of the Working Group on Thermal Regimes of the Section on Ice Research and Engineering of the International Association for Hydraulic Research, is a comprehensive overview of frazil ice. Starting from the initial nucleation of single frazil ice crystals to the formation of ice covers that may be many kilometers long, the physics and evolution of frazil ice in natural water bodies are described. Laboratory experiments conducted over the last 30 years on frazil ice dynamics and other aspects of frazil are described and classified. A physically based, quantitative model that describes the dynamic evolution of the crystal size distribution function is presented. In addition, the development of numerical models of frazil ice in oceans and rivers is discussed and their results described. This report serves as a review of the state of the art of the present understanding of frazil, and the extensive references are a comprehensive resource.

**14. SUBJECT TERMS**

| Anchor ice | Frazil ice dynamics | Ice nucleation | Secondary nucleation |
|---|---|---|---|
| Frazil ice | Grease ice | Numerical modeling | Slush ice |

**15. NUMBER OF PAGES**
52

**16. PRICE CODE**

| 17. SECURITY CLASSIFICATION OF REPORT | 18. SECURITY CLASSIFICATION OF THIS PAGE | 19. SECURITY CLASSIFICATION OF ABSTRACT | 20. LIMITATION OF ABSTRACT |
|---|---|---|---|
| UNCLASSIFIED | UNCLASSIFIED | UNCLASSIFIED | UL |